Cytoprotective Role of PARP inhibition, Akt Activation and Mitochondrial Protection in Oxidative Stress

Antal Tapodi

Institute of Biochemistry and Medical Chemistry

Faculty of Medicine

University of Pécs

Ph.D. Program leader: Prof. Balazs Sümegi, DSc.

Project leader: Ferenc Gallyas Jr., Ph.D.

Contents

Abbreviations

PARP …….. poly(ADP-ribose) polymerase

C1 and N3 ..... mammalian expression vector construct
FCS ..... fetal calf serum
GFP ..... green fluorescent protein
GSK..... glycogen synthase kinase
JC-1 ..... 5,5,6,6-tetrachloro-1,1,3,3-tetraethylbenzimidazolylcarbocyanine iodide
MEM ..... minimum Eagle's medium
MTT ..... 3-(4,5-dimethylthiazol-2-yl)-2,5-diphenyl-tetrazolium bromide
ECL ..... enhanced chemiluminescence
PAR..... poly(ADP-ribose)
PARP-DBD..... N-terminal DNA binding domain of PARP
PI3-kinase ..... phosphatidylinositol 3-kinase
siRNA ..... small interfering RNA
DR…….Death Receptor

BH ..... Bcl-2 Homology
DD..... Death Domain
MPT ..... Mitochondrial Permeability Transition
ROS..... Reactive Oxygen Species
AIF ..... Apoptosis Inducing Factor
PTPC ..... Permeability Transition Pore Complex
VDAC ..... Voltage Dependent Anion Channel
ANT ..... Adenine Nucleotide Translocase
Smac..... Second Mitochondrial Activator of Caspases
DIABLO ..... Direct IAP-Binding Protein of Low isoelectric point [pI]
IAP ..... Inhibitor of Apoptosis
IM..... Inner Membrane
OM ..... Outer Membrane
$\Delta\Psi$ ..... Mitochondrial Membrane Potential
CsA ..... cyclosporine A
Rh123 ..... Rhodamine 123

DRh123 ..... Dihydrorhodamine 123

Resorufin..... N-acetyl-8-dodecyl-3,7-dihyroxyphenoxazine

HEPES ..... N-2-hydroxyethyl piperazine-N'-2-ethansulfonic acid

PI ..... Propidium Iodide

SCAV……1-hydroxy-2,2,5,5-tetramethyl-2,5-dihydro-1*H*-pyrrol-3-ylmethyl

Introduction.

I. Poly-(ADP-ribose) polymerase (PARP-1)

1. Structure of PARP-1

Until recently, only one type of poly-(ADP-ribose) polymerase (PARP) was thought to exist: the PARP-1. However, the development of mice deficient for the PARP-1 gene has completely changed this view. To date, more than 16 new PARP family members can be found in the human genome (Shall S 2002).

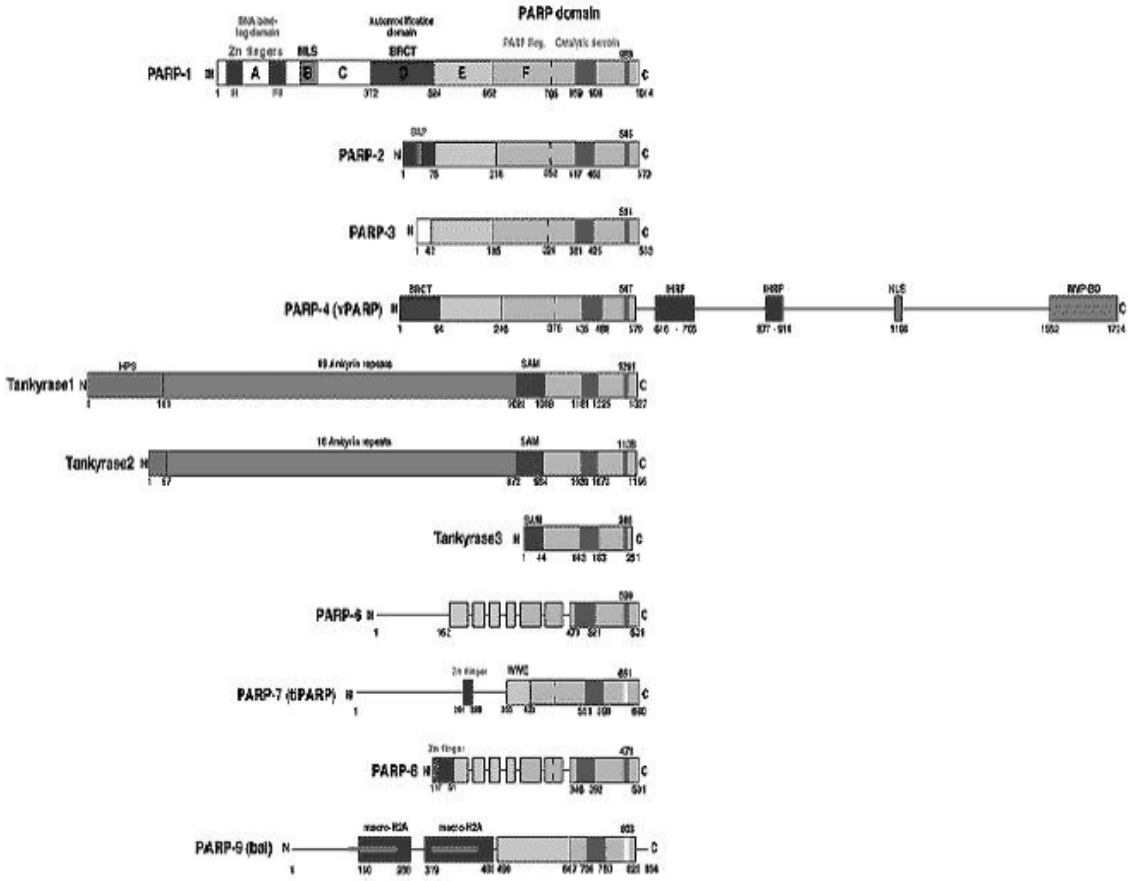

FIGURE 1. The structures of the PARP subclasses.

These new PARPs are structurally distinct from the classical 114 kDa PARP-1 enzyme, and can be classified into several subgroups (Fig. 1) according to their sequence and size. Only limited data are avaliable regarding the physiological roles of these nonclassical PARP family members.

Mammalian PARP-1, a 114 kDa abundant nuclear chromatin associated protein, belongs to a large family of enzymes that catalyzes the transfer of ADP-ribose units from beta-nicotinamide adenine dinucleotide (NAD^+) onto glutamic acid residues of nuclear protein acceptors. The existence of a PARP enzyme was first reported nearly 40 years ago. PARP-1 is one of the best-characterized examples of this family. The activity of PARP-1 is strongly stimulated by the presence of nicks and strand breaks in DNA (Alvarez-Gonzalez R 1994). These observations have contributed to the idea that PARP mediates stress-induced signaling and functions in an NAD^+-dependent manner in certain cellular processes (Althaus FR 1990; Althaus FR, 1992). Since then, the biological significance of PARP has been reported in many cellular processes (D'Amours D 1999; Le Rhun Y 1998; Shall S 2000), however, several aspects of the physiological role of PARP-1 is still to be elucidated. Earlier studies using inhibitors of PARP enzymatic activity such as 3-AB and nicotinamide suggested that PARP-1 plays a crucial role in DNA replication, DNA base excision repair, recombination as well as regulation of telomere lenght (Shall S 2000). Other functions proposed for PARP-1 include gene expression, chromatin organization, proliferation and differentiation, cellular NAD^+ metabolism and necrosis. In addition to the PARP-related energetic depletion and suicidal cycle, PARP may have other important functions in modulating cell death. Although highly controversial, PARP (or its cleavage) may have a role in the process of apoptosis (Kaufman SH 1993; Nocholson DW 1995). Several reports demonstrated that peroxynitrite – as well as hydrogen peroxide and various other oxygen derived oxidants and free radicals – can cause apoptosis in a variety of cell types (Salgo MG 1995; Bonfoco E 1995; Lin KT 1995). It appears that sustained exposure or low levels of peroxynitrite cause apoptosis, whereas sudden exposure to high concetrations of peroxynitrite induces cell necrosis. However, the peroxynitrite-induced apoptosis, in all cell types studied so far, cannot be attenuated by pharmacological

inhibitors of PARP or PARP-/- phenotype (Virag L 1998; Leist M 1997; Wang ZQ 1997; O'Connor M 1997). PARP-1 also serves as a marker for the onset of apoptosis, after which it is cleaved by caspases into DNA-binding and catalytic fragments (Gu Y 1995; Tewari M 1995).

PARP-1 is found in all multicellular lower and higher eukaryotes studied so far. The structure of the type 1 PARP has been extensively characterized. PARP-1 is a highly conserved multifunctional enzyme consisting of three domains: a DNA-binding domain (DBD) containing a bipartite nuclear localization signal (NLS) which is interrupted by a caspase cleavage site, an automodification domain and a catalytic domain (Fig. 2). Tha catalytic domain is the most highly conserved region of the PARP molecule (Murcia G 1994). The N-terminal DBD of human PARP-1 spans residues 1-373 and has a molecular mass of approximately 42 kDa. This domain contains two zinc fingers (FI and FII) and two helix-turn-helix (HTH) motifs (Gradwohl G 1990; Ikejima M 1990).

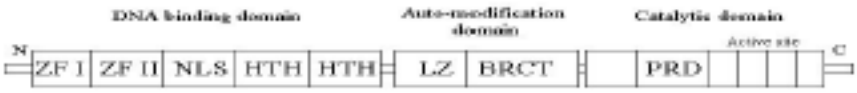

FIGURE. 2 Schematic representation of the PARP-1 map. *Abbreviations: BRCT: BRCA-C-terminal domain; ZF: zinc finger; HTH: helix-turn-helix domain; LZ: leucine zipper; NLS: nuclear localization signal; PRD: PARP regulatory domain.*

Studies have shown that these two zinc fingers are the main stuctures responsible for binding to double-strand breaks (DSBs) or single-strand breaks (SSBs) and for activation of PARP-1 enzyme activity. The moderate non-specific association of PARP-1 with non-damaged DNA has been proposed to depend most probably on the HTH motifs (Thibodeau J 1993). Moreover, the zinc fingers can also act as an interface with various protein partners.

The automodification domain of PARP-1 extends from residues 374 to 525 bearing a leucine zipper (LZ) motif in the N-terminal part and a BRCA1 carboxyl-terminal (BRCT) protein interaction domain in the C-terminal part (Uchida K 1993). Both the LZs and the BRCT domain are well known to be involved in protein-protein interactions (Buch SJ 1990; Callebaut I 1997). Experimental data suggested that the LZs might be responsible for homodimerization of PARP-1 (Kim JW 2000). In addition, the automodification domain contains possible auto-poly(ADP-ribosyl)ation sites implicated in the negative regulation of interactions between PARP-1 and DNA (Duriez PJ 1997; Mendoza Alvarez H 1999).

2. Tissue distribution, expression levels and subcellular localization of PARP-1

The tissue distribution of PARP-1 and its enzymatic activity have been examined in several rat and mouse organs (Ogura T 1999; Menegazzi M 1991). Northern blot analysis and *in situ* hybridization have revealed that PARP-1 gene is constitutively expressed in testis, spleen, brain, thymus, intestine, colon and nasal cavities. Very high levels of PARP-1 were found in lymphoid organs, especially the thymus, in the germinal centers of the spleen and in the Peyer's patches in the ileum, while only very low levels of PARP-1 expression were found in organs such as liver, kidney and heart (Dantzer F 2000). In the central nervous system (CNS), PARP-1 is highly expressed in regions with a high neuronal cell density such as hypocampal neurons of the regions CA1 and 3, granule cells of the dentate gyrus, Purkinje cells of the cerebellar cortex, as well as microglia and astrocytes in several regions (Zucconi G 1992). Interestingly, for non-neuronal cell types, a direct correlation could be observed between cell proliferation and high expression levels of PARP-1. Several studies have shown that an increase in PARP-1 mRNA levels is observed during thymocyte proliferation and upon activation of lymphocytes and peripheral blood mononuclear cells (Menegazzi M 1988; McNerney R, 1989). Moreover, the PARP-1 mRNA level reaches its

peak either in the G1 or the S phases (Wesierska-Gadek J, 2000). The tissue-, cell- and cycle-specific expression pattern of PARP-1 suggests strongly not only that PARP-1 is critical to major cellular functions but also that its expression is modulated through complex transcriptional regulation.

Observation of several different tissues and cell lines using conventional fluorescence microscopy revealed that PARP-1 is exclusively localized to the nucleus (Cocha I 1989). Subsequent studies using either confocal laser scanning microscopy, electron microscopy or cell fractionation experiments showed that PARP-1 is not homogeneously distributed in the nucleus. PARP-1 was shown to be associated with nuclear matrix regions and localized to centromeres during metaphase (Kanai M 2000), while other studies indicated that PARP-1 is found preferentially in nucleoli and defined nuclear bodies (Desnoyers S 1996). Interestingly, PARP-1 was also shown to be associated with actively transcribing nucleolar regions and nuclear bodies. Treatment of cells with RNA synthesis inhibitors caused PARP-1 immunofluorescence to become evenly distributed throughout the nucleus. The association of PARP-1 with actively transcribed regions in the chromatin strongly implies a role for PARP-1 in transcription. Surprisingly, treatment with DNA synthesis inhibitors did not change the distribution of PARP-1 in the nucleus.

3. PARP-1 $^{-/-}$ mice

In recent years, several laboratories developed mice deficient for the PARP-1 gene. The three different knockout mice were created by interruption of either exon 2, exon 4 or exon 1 of the PARP-1 gene in mice (Wang ZQ 1997; Trucco C 1998; Masutani M 1999). Surprisingly, PARP-1 $^{-/-}$ mice from all three different laboratories are viable and fertile. Furthermore, they did not show any phenotypic abnormalities such as organ failures as one would have clearly expected from the data obtained using inhibitors of PARP enzyme

activity and taking into account that knockouts of genes like XRCC1, DNA polymerase-β or APE, which play a crucial role in the BER pathway are lethal (Xanthoudakis S 1996; Tebbs RS 1999; Sugo N 2000). Indeed, carefully designed studies with PARP-1$^{-/-}$ cells clearly demonstrated that PARP-1 is dispensable and not essential for replication, repair of DNA damage or apoptosis *in vitro* or *in vivo* (Ha HC 1999; Vodenicharov MD 2000). Interestingly, recent studies using PARP-1$^{-/-}$ mice showed that they were protected against lipopolysaccharide (LPS)-induced septic shock, collagen-induced arthritis, streptozotocin-induced diabetes, hemorrhagic shock and neuronal damage induced by transient middle cerebral artery occlusion (MCAO) and 1-methyl-4-phenyl-1,2,3,6-tetrahydropyridine (MPTP), indicating that PARP-1 plays a crucial role in inflammatory and neurodegenerative disorders and is involved in the pathogenesis of these events (Szabo C 1997; Pieper AA 1999; Oliver FJ 1999; Mandir AS 1999; Eliasson MJ 1997; Liaudet L 2000).

4. Physical function of PARP

Activation of PARP-1 was proposed to be one of the earliest responses of mammalian cells to genotoxic stress (Lindahl T 1995). The enzymatic activity of PARP-1 is strongly stimulated *in vitro* and increased by 10- to 500-fold in the presence of nicks and double strand breaks in DNA (D'Amours D 1999). These observations have led to the idea that PARP-1 might act as a „molecular nick sensor", thereby mediating stress-induced signaling in the presence of DNA lesions in an NAD^+-dependent manner to downstream effectors involved in coordinating the cellular response to DNA damage (Althaus FR 1992). The „molecular nick sensor" signaling model proposes that PARP-1 recognizes and rapidly binds to DNA strand breaks through its zinc fingers and in turn, the catalytic domain of PARP-1 is allosterically activated and starts to synthesize complex branched poly-(ADP-ribose) chains, resulting in automodification of PARP-1 itself and probably to extensive

modification of histones at sites of DNA strand breaks. Modification of chromatin proteins and PARP-1 itself might then subsequently act as a strong signal that may rapidly recruit other DNA damage-signaling molecules.

More than 40 nuclear chromatin-associated proteins have been implicated the function as a substrate for PARP-1 and to be modified by poly-(ADP-ribose) chains *in vivo*. Target proteins include topoisomerase I and II, histones, p53 and high-mobility group proteins (Kasid UN 1989; Scovassi AI 1993; Wesierska-Gadek J 1996; Boulikas T 1991). In intact organisms, PARP-1 itself is the predominant acceptor of poly-(ADP-ribose). Except for PARP-1 itself, data about modifications of proteins by PARP-1 *in vivo* should, however, be very cautiously interpreted. Despite intense studies in the last 30 years, neither specific glutamic acid residues functioning as poly-(ADP-ribose) acceptor sites nor any specific poly-(ADP-ribosyl)ation motifs could be identified *in vitro*. Moreover, only a few of the proposed substrates of PARP-1, such as p53, topoisomerase I and histone 1 have been shown to directly interact with PARP-1 (Kumari SR 1998; Bauer PI 2001). One has also to stress that the physiological consequences of poly-(ADP-ribosyl)ation of the substrates are in most cases unknown. Lindahl and collegues (Lindahl T 1995) have even proposed that the minor degree of modification of poly-(ADP-ribose) acceptor proteins could be explained as an artificial side reaction *in vitro*.

5. Pharmacological inhibition of PARP-1 in mice

Current strategies aimed at limiting free radical-mediated and oxidant-mediated cell/organ injury include agents that catalyze superoxide or peroxynitrite, or inhibit the induction or activity of the inducible NO synthase. Less attention has been directed to strategies that interfere with intracellular cytotoxic pathways initiated by nitrogen- or oxygen-derived free radicals or their toxic derivatives. Direct and indirect experimental evidence presented in

several papers supports the view that peroxynitrite-induced DNA strand breakage and PARP activation importantly contribute to the pathophysiology of various forms of inflammation.

Pharmacological inhibition of PARP, either with 3-AB (Szabo A, 1998, Shock) or with the potent, novel PARP inhibitors 5-iodo-6-amino-1,2-benzopyrone (Szabo C 1997; Bauer PI 1995) improves survival rate in mice challenged with high dose endotoxin. Also, several recent studies compared the survival times of wild-type and PARP-deficient mice in response to high dose endotoxin, and compared the degree and nature of liver damage in the two experimental groups. In one study, all PARP-deficient animals survived high dose (20 mg/kg) LPS-mediated shock, which killed 60 % of wild-type animals (Kuhnle S 1999). Similar results were obtained by another independent group, led by DeMurcia (Oliver FJ 1999). Szabo C and his group reported that 100% mortality in the wild-type group and less than 50 % mortality in the PARP-deficient animals was observed at 48 h after intraperitoneal injection of high dose (120 mg/kg) E. coli endotoxin. Moreover, LPS-induced necrotic liver damage was significantly reduced in the PARP-deficient mice (Kuhnle S 1999). In contrast, when apoptotic liver damage was induced via injection of low concentrations of LPS (30 mg/kg) into D-galactosamine-sensitized mice, or via activation of hepatic cell death receptors, PARP-deficient animals were not protected. Thus, PARP activation is involved in systemic LPS toxicity, while it plays a minor role in apoptotic liver damage mediated by tumor necrosis factor or CD95.

All of the above-described experiments utilized bacterial components, such as endotoxin or hemorrhage and resusciation. It is generally believed that sepsis induced by live bacteria is more appropriate in mimicking the human septic condition. In a preliminary study, Szabo et al (in: PARP as a therapeutic target) compared the survival rates of wild-type and PARP-deficient mice to cecal ligation and puncture (CLP), a commonly used

model of polymicrobial sepsis. They found that CLP-induced death was delayed in the PARP-deficient mice when compared with wild type animals. The beneficial effects of PARP inhibition in bacterial sepsis were also confirmed in a model of sepsis induced by live E. coli sponge implantation in pigs. Pharmacological inhibition of PARP provides marked hemodynamic improvements and massive survival benefit (Marton A 2001).

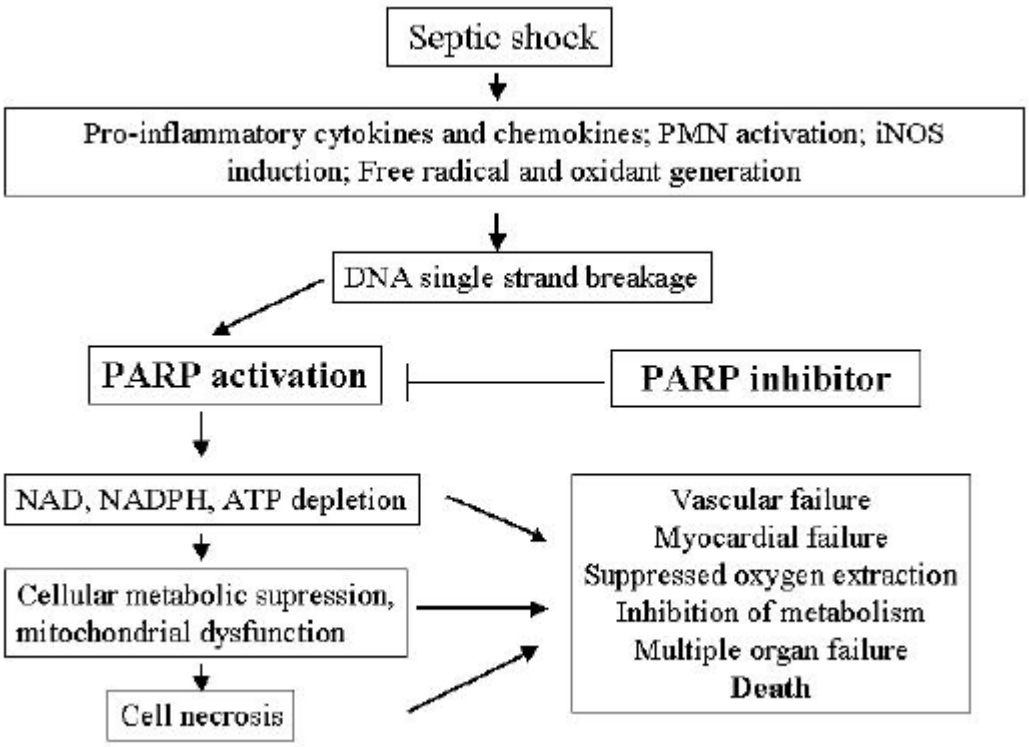

FIGURE. 3 Overview of the connection between septic shock, PARP activation and inflammatory mechanisms. *In sepsis LPS induces the overproduction of pro-inflammatory cytokines and chemokines. The PMN-cell activation and the induction of iNOS leads to free radical and oxidant generation. These agents cause ssDNA breaks and activation of PARP. PARP activation leads to energy depletion, cellular metabolic supression, mitochondrial dysfunction and cell necrosis. After all these processes cause failures of several systems and subsequent death. PARP inhibitors can interfere in a relatively early stage of this process.*

Based on these observations, one can conclude that, in response to pharmacological inhibition or genetic deletion of PARP, the improved hemodynamic status in shock and sepsis is due to improved vascular function and, possibly, the improved cellular energetic

status in some organs. These improvements, in turn, result in an overall survival benefit in this condition (Fig. 3).

Moreover, in the past few years an increasing number of reports have appeared about the importance of the PI3-kinase/Akt and MAPK pathways in LPS-induced inflammatory mechanisms (Bozinovski S 2002; Guha M 2002; Ozes ON 1999). Recent evidence suggests that activation of PI3-kinase, a ubiquitous lipid-modifying enzyme, may modulate positively acting signaling pathways and inhibition of LPS-induced MAPKs activation may play crucial role in the attenuation of endotoxin-induced inflammatory responses due to the modulation of transcription factors.

II.The role of PARP in oxidative stress

Under several pathological conditions, reactive oxygen species-induced damages play important roles in pathogenesis (1–3). High levels of reactive oxygen species are generated from a variety of sources such as the xanthine oxidase system (1), the leakage of electrons from the mitochondrial respiratory chain (2, 4), the cyclooxygenase pathway of arachidonic acid metabolism (3, 5), and the respiratory burst of phagocyte cells (6, 7), and they can cause DNA damage-generating singlestranded DNA breaks (8). Poly(ADP-ribose)polymerase (PARP-1,2 EC 2.4.2.30) is a multifunctional nuclear enzyme (9) that is activated by DNA strand breaks and catalyzes the covalent coupling of branched chains of ADP-ribose units to various nuclear proteins such as histone proteins and PARP-1 itself. PARP-1 is involved in chromatin remodelling, DNA repair, replication, transcription, and the maintenance of genomic stability by, in part, poly(ADP-ribosyl)ation (9). With moderate amounts of DNA damage, PARP-1 is thought to participate in the DNArepair process (10, 11). However, oxidative stress, which induces a large amount of DNA damage, can cause excessive activation of PARP-1, leading to depletion of its substrate

NAD^+; and in an effort to resynthesize NAD^+, ATP is also depleted, resulting in cell death as a consequence of energy loss (12–15). PARP inhibitors show pronounced protection against myocardial ischemia (16), neuronal ischemia (17, 18), acute lung inflammation (19), acute septic shock (20), zymogen-induced multiple organ failure (21), and diabetic pancreatic damage (22–24), providing evidence for the role of excessive PARP-1 activation in cell death. It is believed that by preventing excessive NAD^+ and ATP utilization, PARP inhibitors protect cells against oxidative damage, but some recent data suggest a more complex mechanism for the cytoprotection (25, 26).

III. Akt activation and cytoprotection

1. The phosphoinositide 3-kinase/Akt signaling pathway

The phosphoinositide 3-kinases (PI3Ks) are a conserved family of signal transduction enzymes that are involved in regulating cellular proliferation and survival (16, 17). More specifically, the PI3Ks and the downstream serine/threonine kinase Akt (also known as protein kinase B) regulate cellular activation, inflammatory responses, chemotaxis, and apoptosis (17). PI3K is an enzyme complex composed of 4 known isoforms (α, β, γ and ζ) and a catalytic p110 subunit. The latter also consists of α, β and ζ isoforms, and is associated with the p85 regulatory subunit to form the type 1A PI3K, whereas the p110 γ subunit binds to p101 adapter protein to comprise the Type 1B PI3K. Type 1A PI3K is activated by tyrosine phosphorylation, whereas p110 γ is activated by engagement of Gi protein coupled receptors (18). The p110 γ PI3K plays a central role in inflammation and chemotaxis (19). Phosphorylated lipids are induced in membranes during signaling events (19). PI3K catalyzes the conversion of phosphatidylinositol 4,5 biphosphate PI(4,5)P3 to PI(3,4,5)P3. Signaling proteins with pleckstrin homology domains bind to PI(3,4)P2 or

PI(3,4,5)P3(16). The interaction of pleckstrin homology domains on signaling proteins with PI(3,4)P2 or PI(3,4,5)P3 can modulate signaling and the intracellular localization of the signaling protein. Some examples of signaling proteins that interact with PI(3,4)P2 and/or PI(3,4,5)P3 include phosphoinositide-dependent kinase-1 (PDK1), PDK2, and Akt. PDK activates Akt by phosphorylation of Ser308 and Thr473 (17). The phosphorylated Akt modulates cell cycle entry, growth and survival (17).

2. The PI3K system as a negative regulator of inflammatory processes

Recent evidence indicates that the PI3K/Akt signaling pathway may be an endogenous negative feedback or compensatory mechanism that serves to limit proinflammatory and apoptotic events in response to injurious stimuli (Fig. 4) (7, 20). Guha and Mackman (20) have reported that the „PI3K-Akt pathway imposes a braking mechanism to limit the expression" of proinflammatory mediators in LPS-treated monocytes. Fukao et al. (21) have reported that p85! knockout mice showed impaired clearance of enterobacteria injected into the peritoneal cavity; however, this study did not examine morbidity or mortality in the p85 knockout model. Fukao and Koyasu (22) have reviewed the role of PI3K in the regulation of Toll-like receptor (TLR)Y mediated inflammatory responses. They concluded that PI3K may be an endogenous negative feedback regulator that is crucial to the maintenance and integrity of the immune system (22). They also concluded that PI3K was important in maintaining the balance between in vivo Th1 versus Th2 responses (22). These same investigators hypothesized that the BPI3K-mediated machinery could be an ideal therapeutic target for certain proinflammatory and/or septic diseases (22).

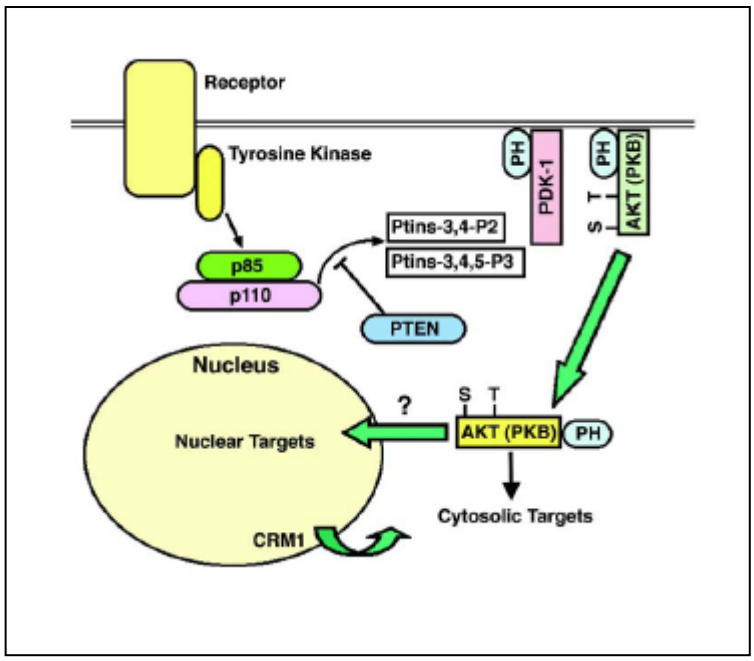

FIGURE 4 Model of Akt activation

Bommhardt et al. (23) have reported that mice that constitutively overexpress active Akt in their lymphocytes showed decreased lymphocyte apoptosis, a Th1 cytokine propensity, and a marked improvement in survival outcome in response to CLP-induced sepsis. Martin et al. (24) have reported that the PI3K/Akt pathway differentially regulates IL-10 and IL-12 production in response to endotoxin through inhibition of glycogen synthase kinase-1 (GSK3). These investigators speculated that the PI3K/Akt/GSK3 pathway „could potentially serve as a therapeutic target against sepsis or other inflammatory diseases" (24). Woodgett and Ohashi (25) have reviewed the work of Martin and colleagues (24). These authors noted the importance of understanding how the TLR and PI3K pathways serve to balance proinflammatory and antiinflammatory responses, and by doing so, they maintain homeostasis and the integrity of the immune response (25). Of potentially greater significance, Woodgett and Ohashi stated that it is important to understand how TLR signaling is connected with the myeloid differentiation factor 88 (MyD88)-IL-1 receptor associated kinase pathway versus the PI3K-Akt-GSK3 pathway (25).

Our previous works demonstrated that PARP inhibitors induced the phosphorylation and activation of Akt in the liver, lung, and spleen of lipopolysaccharide-treated mice, raising the possibility that the protective effect of PARP inhibition can be mediated through the PI3-kinase/Akt pathway (30). Our data show that LPS induces a different extent of MAP kinase activation in different organs, which can activate AP-1 and NF-κB transcription factors in a tissuespecific manner. Activation of these transcription factors induces activation of proinflammatory genes that are most likely responsible for the tissue damage during septic shock. PARP-1 inhibitors beside their well known effect of inhibiting NAD^+ and ATP depletion, influence LPS-induced transcription factor activation and gene expression. These effects of PARP-1 inhibitors are mediated by the activation of the PI3-kinase/Akt pathway, which can inhibit MAP kinase activation and can attenuate transcription factor activation and inflammatory tissue damage (Fig. 5) in a tissue-specific manner.

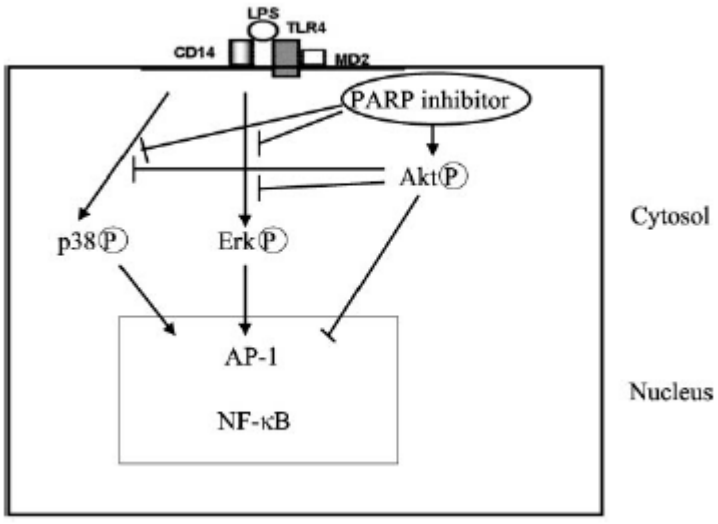

FIGURE 5. Schematic representation of the effect of 4-hydroxyquinazoline on Akt and MAPK activation and NF-_B and AP-1 activation. *Binding of LPS to the CD14 and TLR4/MD2 complex activates the MAPK pathways. PARP-1 inhibitor directly or indirectly activates the PI3-kinase/Akt pathway and inactivates the ERK1/2 and p38 MAPKs. Activation of Akt via PARP-1 inhibition can also inactivate these kinases. Inactivation of*

nuclear transcription factors (NF-κ_B, AP-1) is the consequence, at least partially, of the aforementioned processes.

3. The role of PI3K/Akt system in oxidative injuries

Several protein kinase cascades and inflammatory reactions have recently become established as part and parcel of any external stress-related tissue injury such as ischemia-reperfusion, and other oxidative, metabolic, toxic as well as infectious insults. Previous results indicate that the growth-factor-associated kinase Akt (protein kinase B) is phosphorylated following ischemia-reperfusion in cardiomyocytes in a phosphoinositol-3-kinase (PI3-kinase)-dependent manner (11). PI3-kinase pathway is one of several signal transduction pathways implicated in cell survival (12,13). Our previous works demonstrated that PARP inhibitors induced the phosphorylation and activation of Akt in the liver, lung, and spleen of lipopolysaccharide-treated mice, raising the possibility that the protective effect of PARP inhibition can be mediated through the PI3-kinase/Akt pathway (30). Akt, in turn, phosphorylates a number of downstream targets leading to the inactivation of glycogen synthase kinase-3β (GSK-3β), the pro-apoptotic Bcl-2 family member Bad (14), caspase-9 (15), Forkhead transcription factor (13), as well as to the activation of nuclear factor-κB (NF-κB) (16), p70 ribosomal S6 kinase and endothelial nitric oxide synthase (eNOS) (17,18).

Inactivation of GSK-3β will allow glycogen synthase to build up cellular glycogen stores, eukaryotic initiation factor 2B (eIF2B) to launch the synthesis of various proteins as well as cyclin D1 to facilitate cell cycle progression (19). Two Bad molecules constituting a homodimer can contribute to the release of cytochrome c from the external side of the inner mitochondrial membrane into the cytoplasm, where the free cytochrome c triggers apoptotic cell death with the participation of caspase-9. Bad homodimer formation is prevented either through the dimerization with Bcl-2 anti-apoptotic molecule or by Bad

phosphorylation, for instance by Akt, directing it toward degradation (20). Moreover, endothelial nitric oxide synthase is activated by Akt forms nitric oxide causing vasorelaxation (17,18). The overall impact of Akt action is thus a remarkable antiapoptotic effect, metabolic adjustment and vasodilation, each of which inevitably promotes cell survival.

Wortmannin is a fungal metabolite having a sterol-type structure, passes into cells by simple diffusion, and irreversibly binds to and blocks the 110-kDa catalytic subunit of PI3-kinase (21,22). Previous studies have shown that wortmannin inhibits superoxide release, adherence and chemotaxis of polymorphonuclear leucocytes (23-25). However, the effects of wortmannin have not yet been studied in myocardial ischemia/reperfusion injury in the presence of PARP inhibitors. LY294002 is another potent PI3-kinase inhibitor.

4. The PI3K/Akt systemis mediated through cholesterol-rich plasma membrane rafts during oxidative stress

Reactive oxygen species (ROS) generated during pathological events, such as inflammation and ischemia-reperfusion, activates both proapoptotic and antiapoptotic signaling programs in endothelial cells. Cholesterol-rich, plasma membrane rafts serve as platforms for organizing and integrating signaling transduction processes. These membrane regions play a mechanistic role in H2O2-induced responses. If an aortic endothelial cell line is exposed to a 500-microM bolus of H2O2 showed progressive activation of caspase 3 and an increase in the number of TUNEL-positive cells. Pretreatment with either wortmannin or PD 098059 heightened these apoptotic responses, demonstrating that both PI3 kinase/Akt and ERK1/2 serve as signaling mediators to alleviate H2O2 cytotoxic effects. However, the raft structures are destroyed by methyl-beta-cyclodextrin (CD) or filipin, H2O2-induced phosphorylation of Akt and ERK 1/2 are attenuated, while caspase 3 and the number of TUNEL positive cells are enhanced in CD-pretreated cells exposed to H2O2.

Reconstitution of raft domains restored H2O2-induced Akt and ERK1/2 phosphorylation, which is concomitant with reduction of caspase 3 activation and DNA fragmentation. Taken together, these discoveries suggest that plasma membrane compartments rich in cholesterol participate in signal transduction pathways activated by oxidative stress.

IV. Mitochondrial permeability transition

1. MPT

MPT is a major event in physiological as well as pathological cell death, and not surprisingly, it is regulated at multiple levels (Zamzami et al., 1996). MPT can be induced by multiple pro-apoptotic second messengers (Fig. 6.), including Ca^{2+}, reactive oxygen species (ROS), lipid messengers (e.g. ceramide and ganglioside GD3) and stress kinases. In addition it is facilitated by pro-apoptotic proteins from the Bcl-2 family, and is inhibited by anti-apoptotic

Bcl-2-like proteins. MPT might involve the formation of protein-permeable pores by oligomers of Bax and Bak (two pro-apoptotic proteins of the Bcl-2 family), as well as the transient or permanent opening of a variety of different channels, including those contained in the permeability transition pore complex (PTPC), such as the voltage-dependent anion channels (VDAC) in the outer membrane and the adenine-nucleotide translocase (ANT) in the inner membrane. In addition to PTPC-dependent mechanisms, recent findings suggest that apoptotic proteins such as cytochrome *c* can be released from the mitochondria by as yet

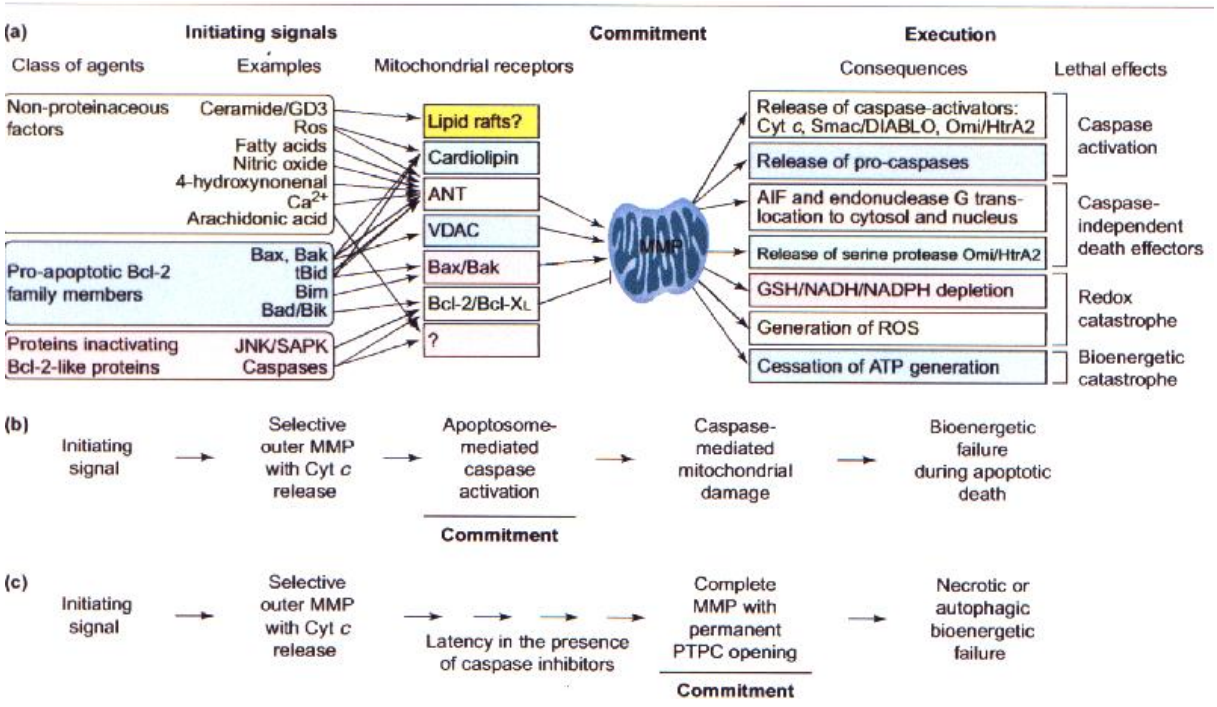

FIGURE .6. The importance of mitochondrial membrane permeabilization in apoptosis. *Different apoptogenic molecules act on a variety of tenetively identified MPT regulator. MPT has several functional consequence resulting in cell death via both caspase-dependent and caspase-independent death effectors.*

undetermined mechanisms that do not involve formation of PTPC. Furthermore, different K^+-selective channels in the inner membrane might control the volume of the mitochondrial matrix and ultimately the intactness of mitochondrial membranes. Moreover, inner-membrane uncoupling proteins (UCPs), which regulate the transmembrane proton gradient and the production of ROS and ATP, are increasingly being recognized for their roles in modulating cell death. Irrespective of the exact mechanism of MPT, it appears that this event can mark the 'point of no return' in the cell death process.

2. Mechanism of mitochondrial permeability transition (MPT)

Mitochondria are organelles with two well-defined compartments: the matrix, surrounded by the inner membrane (IM), and the intermembrane space, surrounded by the outer membrane (OM). The IM is folded into numerous christae, which greatly increases its surface area. It contains the protein complexes from the electron transport chain, the ATP

synthase and the adenine nucleotide translocator (ANT). To function properly, the IM is almost impermeable to the various metabolites in physiological conditions (except for the those that have regulated transport mechanism), thereby allowing the respiratory chain to create an electrochemical gradient ($\Delta\Psi$). The $\Delta\Psi$ results from the respiration-driven, electron-transport-chain-mediated pumping of protons out of the inner membrane and is indispensable for driving the ATP synthase which phosphorylates ADP to ATP. ATP is then exported in exchange for ADP by the ANT. The OM in normal conditions is permeable to solutes up to about 5,000 Da. Thus, whereas the matrix space contains a highly selected set of small molecules, the intermembrane space is chemically equivalent to the cytosol with respect to low-molecular-weight solutes. The OM permeabilization involves the release of proteins which are normally confined to the intermembrane space, including cytochrome c, Smac/DIABLO, Omi/HtrA2 and AIF. The IM permeabilization may occur in a 'step-wise' manner (Green and Reed 1998; Bernardi 1999), with increasing permeability of solutes up to about 1,500 Da (Fig. 7.), and is manifested as the dissipation of the proton gradient responsible for the trans-membrane potential ($\Delta\Psi$), an extrusion of small solutes (such as calcium or glutation), or an influx of water and sucrose (which, in sucrose-containing media, leads to large-amplitude swelling of the matrix).

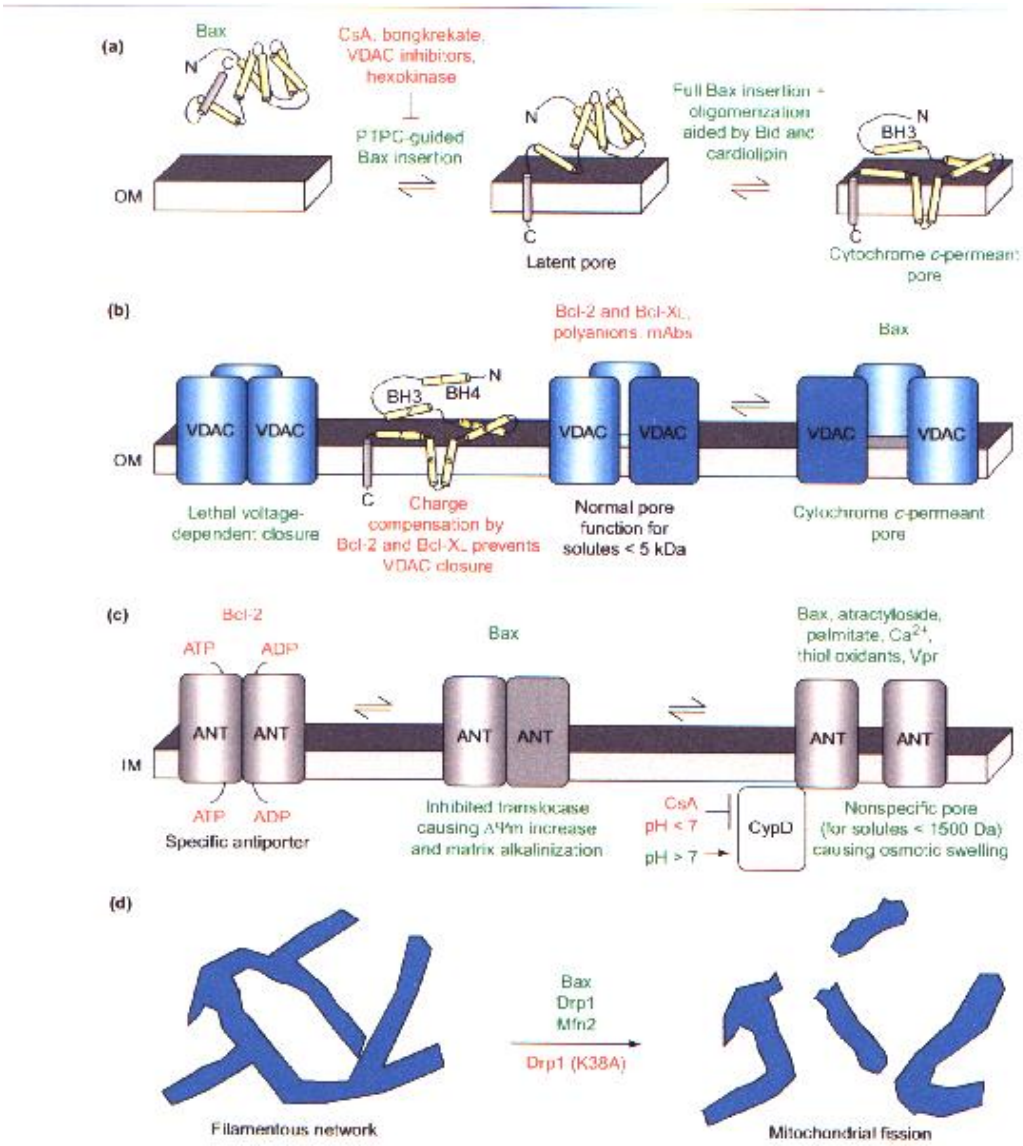

FIGURE 7. Possible mechanisms of mitochondrial permeability transition (MPT). *The precise mechanisms of MPT are still unsolved and might depend on the initiating stimulus. Inhibitors of permeabilization are denoted in red and inducers are in green. Adenine-nucleotide translocase (ANT), voltage-dependent anion channel (VDAC) and cyclophillin D (CypD), as well as Bcl-2-like proteins, might be organized in higher-order molecular complexes, such as the so-called permeability transition pore complex (PTPC).*

3. Amiodarone

Amiodarone (2-butyl-3-benzofuranyl 4-[2-(diethylamino)-ethoxy]-3,5-diiodophenyl-ketone hydrochloride) is one of the most effective antiarrhythmic drugs and is frequently used in the clinical practice for treating ventricular and supraventricular

arrhythmias. It is a class III antiarrhythmic agent, prolonging action potential duration whose effect may involve blocking of β-adrenergic receptors, sodium channels, and L-type calcium channels (Singh and Vaughan Williams, 1970; Nokin et al., 1983; Nattel et al., 1987; Varro et al., 1996). It may also have a role in preventing mortality after myocardial infarction (Julian et al., 1997). Despite its effective antiarrhythmical properties, the use of amiodarone is often limited by its toxic side effects, including thyroid dysfunction, liver, and pancreas fibrosis (Amico et al., 1984; Martin and Howard, 1985). However, the most severe adverse effect of the drug is pulmonary fibrosis, occurring in up to 13% of the patients receiving the amiodarone in doses higher than 400 mg/day (Martin and Rosenow, 1988). The etiology of the amiodarone-induced pulmonary toxicity is unknown.

As previously mentioned high levels of reactive oxygen species (ROS) are generated from a variety of sources such as the xanthine oxidase system (4), the leakage of electrons from the mitochondrial respiratory chain (5,7), the cyclooxygenase pathway of arachidonic acid metabolism (6,8), and the respiratory burst of phagocytic cells (9,10), which have deteriorating cellular effects like lipid peroxidation, protein oxidation, enzyme inactivation, DNA strand breaks, and the impairment of several physiological functions, such as blocking of ion channels, restriction of glycolysis, or the facilitation of mitochondrial Ca2+ release (11–13). Calcium overload together with the increased intracellular phosphate concentration (the result of ATP degradation during ischemia) leads to mitochondrial permeability transition (mPT), an opening of a mega pore in the mitochondrial membrane.

In order to understand more exactly the mitochondrial effects of ROS induced injuries we have investigated a novel SOD-mimetic permeability transition inhibitor as an amiodarone derivate (HO-3538) on the apoptotic and necrotic cell death. The effect of amiodarone is due—at least in part—to the inhibition of mitochondrial permeability

transition (MPT) in lower concentrations. However, when administrated in higher concentrations, it induced mitochondrial swelling as well as the collapse of the mitochondrial membrane potential (Dw). N-Desethylamiodarone, the major metabolite of amiodarone— reported by some authors to be the major cause of the amiodarone administration induced toxicity— does not present these biphasic characteristics, with no inhibitory effect on the MPT in lower concentrations and the induction of swelling and the collapse of the 60 membrane potential in higher concentrations. The difference between the effect of amiodarone and N-desethylamiodarone is due to the absence of an ethyl side chain from the amino group of N-desethylamiodarone. This led us to the conclusion that the structural modification of amiodarone can improve its inhibitory effect on MPT as well as its beneficial effect in ischemia- reperfusion injuries. Considering the advantages of amiodarone, a lot of effort has been made in the past decade to improve pharmacokinetic properties of amiodarone, mainly by chemical alterations of the original molecule such as synthesis of monoiodo derivatives, introduction of carboxymethoxy side chain instead of tertiary amine or substitute the original n-butyl group for an isobutyl ester.

We got from Prof. Hideg and his co-workers numerous paramagnetic and diamagnetic amiodarone derivates, synthetised by them, and screened their effect on the mitochondrial permeability transition (Kalali at al., 2005). In this study, we analyzed the effect of HO-3538, the most effective novel amiodarone analogue, in which an ethyl side chain is substituted with 1-hydroxy-2,2,5,5-tetramethyl-2,5-dihydro-1*H*-pyrrol-3-ylmethyl (SCAV) that has been described to possess free-radical scavenging activity (Krishna at al,, 1998) on the permeability transition *in vitro* and in cultured cells, as well as on ischemia-reperfusion in Landendorff-perfused rat hearts, also. This amiodarone analogue can be new leading compound among the experimental amiodarone analogues with the same or enhanced efficiency of amiodarone, but with less side effects.

Objectives.

1. Several study have shown that the different PARP inhibitors improve the survival of cells in oxidative stress. Is this cytoprotection achieved via direct attenuation of PARP-1 activation or decrease of the activity of other ADP-ribosylating enzymes?
2. It is widely accepted fact that the cytoprotective effects of PARP inhibition in oxidative stress are based on the prevention of NAD^+ and ATP depletion. Is this protection mediated only through the preservation of the energetics of cells alone or there might be present other mechanisms as well?
3. Our previous works demonstrated that amiodarone has a biphasic effect on mPT; it protected the mitochondria from mPT at low concentration although it induces a CsA independent mitochondrial swelling at higher concentration. Can appropriate substitution of amiodarone suppress the mPT inducing effects of the drug while maintaining its protective effects on mitochondria?
4. After screening of many amiodarone derivates we selected a novel amiodarone analogue (HO-3538), in which an ethyl side chain was substituated with a SOD-mimetic one. What are the beneficial effects of the combination of mPT inhibition and free-radical scavenging in ischemia-reperfusion and oxidative stress?

Materials and Methods.

Materials

PI3-kinase inhibitors LY 294002 and wortmannin, PARP-1 inhibitor PJ-34, protease inhibitor mixture, and all of the chemicals for cell cultures were purchased from Sigma. Fluorescent dyes JC-1, fluorescein-conjugated annexin V, and propidium iodide were from Molecular Probes. The following antibodies were used: anti-phospho- Akt (Ser473) and anti-phospho-GSK3_(Cell Signaling Technology, Beverly, MA); anti-PAR and anti-PARP (Alexis Biotechnology, London, U.K.); anti-actin, anti-mouse IgG, and anti-rabbit IgG (Sigma). Cyclosporin Awas from Biomol Research Laboratories, Inc. (Plymouth Meeting, PA, USA); rhodamine 123 (Rh123) and carboxy-H2DCFDAwere from Molecular Probes (Eugene, OR, USA), anti-cytochrome c monoclonal antibody was from Pharmingen (San Diego, CA, USA), anti-apoptosis-inducing factor (AIF) polyclonal antibody was from Oncogene (San Diego, CA, USA), HO-3538 (2-methyl-3-(3,5-diiodo-4-{2-[Nethyl, N-(1-hydroxy-2,2,5,5-tetramethyl-2,5-dihydro-1H-pyrrol- 3-ylmethyl) ethyl]}oxybenzoyl)benzofurane · 2HCl salt) was produced as described previously [27] all other compounds were from Sigma Chemical Co. (St. Louis, MO, USA) unless otherwise stated.

Cell Culture

WRL-68 human liver cells, H9C2 mouse cardiomyoblast, Jurkat cells were from the American Type Culture Collection (Wesel, Germany). The cells were maintained as monolayer adherent culture in minimum Eagle's medium, Dulbecco's modified Eagle's medium containing 1% antibiotic-antimycotic solution and 10% fetal calf serum (MEM/ FCS) in a humid 5% CO2 atmosphere at 37 °C. Jurkat cells were maitained in RPMI.

Transdominant Expression of the DNA-binding Domain of PARP

The coding region of the N-terminal DNA-binding domain of PARP (PARP-N214, amino acid residues 1–214 (34)) was amplified by PCR and cloned in-frame into pEGFP-C1/N3 vectors (Clontech) after cutting with HindIII and EcoRI restriction enzymes (Fermentase, Vilnius, Lithuania). For enabling active nuclear transport of the green fluorescent protein (GFP)-tagged PARP-N214, the nuclear localization signal was added to the N terminus of the PARP-N214 sequence using PCR primers coding for the nuclear localization signal sequence. The recombinant pPARPGFP-C1/N3 vectors were purified by a plasmid purification kit (Qiagen, Valencia, CA) and utilized for transient transfection of WRL-68 cells using Lipofectamine 2000 (Invitrogen) according to the manufacturer's protocol. For an effective transdominant expression of PARP-DBD, the transfection step was repeated 48 h after the first transfection, and the experiments on the cells were performed 40 h after the second transfection. *Suppression of PARP-1 Expression by siRNA Technique*—WRL-68 cells were transiently transfected with siRNA designed for PARP suppression by the manufacturer (Santa Cruz Biotechnology, Santa Cruz, CA) in Opti-MEM I Reduced Serum Medium (Invitrogen) using Lipofectamine 2000. For an effective suppression of PARP, the transfection step was repeated twice with a 48-h interval between the transfections, and the experiments on the cells were performed 40 h after the third transfection.

Cell Viability Assay

The cells were seeded into 96-well plates at a starting density of 104 cell/well and cultured overnight beforeH2O2 and different inhibitors modulating the effect of theH2O2 were added to the medium at a concentration and composition indicated in the figure legends. After 3 h of treatment, the medium was removed, and fresh MEM/FCS containing 0.5% of the water-soluble yellow mitochondrial dye MTT was added. Incubation was continued for an additional 3 h, and the MTT reaction was terminated by adding HCl to the medium at a final concentration of 10 mM. The amount of water-insoluble blue formasan dye formed from MTT was proportional to the number of live cells and was determined with an Anthos Labtech 2010 enzyme-linked immunosorbent assay reader at 550 nm wavelength after dissolving the blue formasan precipitate in 10% SDS. All experiments were run in at least four parallels and repeated three times.

Western Blot Analysis

The cells were seeded and treated as for the cell viability assay. After 1 h of treatment, the cells were harvested in a chilled lysis buffer of 0,5 mM sodium metavanadate, 1 mM EDTA, and protease inhibitor mixture in phosphate-buffered saline. The proteins were precipitated by trichloroacetic acid, washed three times with _20 °C acetone, and subjected to SDS-PAGE. Proteins (30 _g/lane) were separated on 12% gels and then transferred to nitrocellulose membranes. The membranes were blocked in 5% low fat milk for 1 h at room temperature, then exposed to the primary antibodies at 4 °C overnight at a dilution of 1:1,000 in blocking solution. Appropriate horseradish peroxidase-conjugated secondary antibodies were used for 2 h at room temperature and a 1:5,000 dilution. Peroxidase labeling was visualized with enhanced chemiluminescence (ECL) using an ECL Western blotting detection system (Amersham Biosciences). The developed films were scanned, and

the pixel volumes of the bands were determined using NIH Image J software. All experiments were repeated four times.

Determination of NAD$^+$ The cells were seeded and treated as for the cell viability assay. All experiments were run in two (for transfection experiments) or three parallels and were repeated twice. Harvesting and sample processing were performed according to Du *et al.* (29). Cellular NAD^+ levels were measured by the microplate version of the enzymatic cycling method using alcohol dehydrogenase exactly as described by Shah *et al.* (36) except for using iodonitrotetrazolium chloride instead of MTT in the assay buffer, the former having the advantage of being water-soluble. The reaction was monitored at 550 nm and was allowed to run for 10 min. A standard curve was generated using known concentrations of NAD^+ for the calculation of the cellular NAD^+ levels. Cellular protein contents of the cell homogenates were determined with the BCA protein assay reagent (Pierce, Rockford, IL, USA) using bovine serum albumin as standard.

Fluorescent Microscopy

Wild type or transfected WRL-68 cells were seeded to poly-L-lysine-coated (2.5–5 μg/cm2) glass coverslips and cultured at least overnight before the experiment. After subjecting the cells to the appropriate treatment (indicated in the figure legends), the coverslips were rinsed twice in phosphate-buffered saline then placed upside down on the top of a small chamber formed by a microscope slide and a press-to-seal silicone isolator filled with phosphate-buffered saline containing 4.5 g/liter glucose and 20 mM HEPES pH 7.4. Cells were imaged with an Olympus BX61 fluorescent microscope equipped with a ColorView CCD camera and analySISR software using a 60 _ objective and epifluorescent illumination. For GFP fluorescence, 450– 490 nm excitation and _520 nm emission (green)

filters were used. For JC-1 fluorescence, the cells were loaded with the dye for 10 min, then the same microscopic field was imaged first with 546 nm bandpass excitation and _590 nm emission (red), then with green filters. Under these conditions we did not observe considerable bleed-through between the red and green images.

Animals

Wistar rats were purchased from Charles River Hungary Breeding Ltd. (Budapest, Hungary). The animals were kept under standardized conditions; tap water and rat chow were provided ad libitum. Animals were treated in compliance with approved institutional animal care guidelines.

Isolation of mitochondria

Rats were sacrificed by decapitation and the mitochondria were isolated from the liver and the heart by differential centrifugation as described by a standard protocol [29]. The only difference among the organs was in the primary homogenization protocol; the liver was squeezed through a liver press, whereas pooled heart tissue from five rats was minced with a blender. All isolated mitochondria were purified by Percoll gradient centrifuging [30], and the mitochondrial protein concentrations were determined by the biuret method with bovine serum albumin as the standard.

Mitochondrial permeability transition

The mPT was monitored by following the accompanying large amplitude swelling via the decrease in absorbance at 540 nm [31] measured at room temperature by a Perkin–Elmer fluorimeter (London, UK) in reflectance mode. Briefly, mitochondria at the concentration of 1 mg protein/ml were preincubated in the assay buffer (70 mM sucrose, 214 mM mannitol, 20 mM N-2-hydroxyethyl piperazine-N′-2-ethanesulfonic acid, 5 mM glutamate, 0.5 mM malate, 0.5 mM phosphate) containing the studied substances for 60 s. Mitochondrial permeability transition was induced by the addition of 60 μM Ca2+ or amiodarone, or HO-3538 at the indicated concentration. Decrease in E540 was detected for 20 min. The results are illustrated by representative original registration curves from at least five independent experiments, each repeated three times using mitochondria prepared from the same liver or pool of rat hearts.

Mitochondrial membrane potential

The membrane potential was monitored by fluorescence of Rh123, released from the mitochondria after the induction of permeability transition at room temperature by using a Perkin–Elmer fluorimeter at an excitation wavelength of 495 and an emission wavelength of 535 nm. Briefly, mitochondria at the concentration of 1 mg protein/ml were preincubated in the assay buffer (70 mM sucrose, 214 mM mannitol, 20 mM N-2-hydroxyethyl piperazine-N′-2-ethanesulfonic acid, 5 mM glutamate, 0.5 mM malate, 0.5 mM phosphate) containing 1 μM Rh123 and the studied substances for 60 s. Alteration of the mitochondrial membrane potential was induced by the addition of HO-3538 at the indicated concentration. Changes in fluorescence intensity were detected for 4 min. The results are illustrated by representative original registration curves from five 837 Z. Bognar

et al. / Free Radical Biology & Medicine 41 (2006) 835–848 independent experiments, each repeated three times using mitochondria prepared from the same liver or pool of rat hearts.

Detection of mitochondrial protein release

Detection of the release of rat heart mitochondrial proapoptotic proteins in vitro was performed as described [31]. Samples from the cuvette were taken 20 min after the induction of the permeability transition by Ca2+, with CsA or HO-3538 present at the indicated concentration, and centrifuged at 13,000 rpm for 15 min. Pellets and the supernatants were analyzed for cytochrome c (cyt-c), AIF, and endonuclease-G (Endo G). Equal amounts of proteins were separated by a 12% polyacrylamide gel for the detection of AIF and Endo G and by an 18% polyacrylamide gel for the detection of cyt-c. The separated protein samples were transferred to a nitrocellulose membrane, appropriate primary and secondary antibodies were applied, and bands were visualized by enhanced chemiluminescence labeling. Results are illustrated by photomicrographs of representative blots of three independent experiments.

Determination of cytochrome c level by high-pressure liquid chromatography (HPLC)

The analysis of cyt-c was performed on a nonporous 33 × 4.6-mm KOVASIL-MS C18 column (Zeochem AG, Uetikon, Switzerland). Separations were carried out on a Dionex HPLC system consisting of a Dionex P 580 lowpressure gradient pump and a Dionex UVD 340S diode array detector (chromatograms were detected at 393 nm). The samples were injected by a Rheodyne 8125 injector equipped with a 20-µl loop. Instrument control and data acquisition were carried out using Chromeleon data management software. The measurements were accomplished using gradient elution. Eluent A consisted of 10:90

acetonitrile:water + 0.1% (v/v) trifluoroacetic acid and eluent B consisted of 90:10 acetonitrile: water + 0.1% (v/v) trifluoroacetic acid. The applied gradient program was the following: 0 to 7 min, from 0% B to 70% B; 7 to 12 min, from 70% B to 100% B; 12 to 12.5 min, from 100% B to 0% B; 12.5 to 14.5 min, 0% B. The flow rate was 1 cm3 · min−1. The column reequilibration was involved in the gradient program. Data acquisition was performed from at least three independent experiments.

Detection of antioxidant effect in cells

H9C2 cells were seeded into 96-well plates at a starting density of 2 × 104 cells/well and cultured overnight. The next day, the cells were exposed for 90 min to 1 mM H2O2 followed by two washings with phosphate-buffered physiological saline solution. The cells were then preincubated for 30 min in fresh medium containing HO-3538 or different antioxidants at the concentration of 10 μM, and 1 μM carboxy-H2DCFDA was added to the medium for a further 1 h incubation. Fluorescence of carboxy-DCFDA oxidized stoichiometrically by the ROS was measured by using a fluorescence ELISA reader (BMG Laboratories, Offenbach, Germany) at excitation and emission wavelengths of 485 and 555 nm, respectively. All experiments were run at least four in parallel and repeated three times.

Caspase activity assay

Jurkat cells (2 × 106) were treated with different concentrations of HO-3538 in the presence or absence of 50μM etoposide for 12 h. The cells were collected by centrifugation, 838 Z. Bognar et al. / Free Radical Biology & Medicine 41 (2006) 835–848 washed twice with ice-cold PBS, resuspended in 50 μl of icecold lysis buffer (1 mM dithiothreitol, 0.05% Nonidet P-40, in 50 mM Tris, pH 7.5), kept on ice for 30 min, and

centrifuged at 13,000g for 15 min at 4°C. Forty micrograms of protein was incubated with 50 μM caspase substrate (Ac-DEVD-AMC) in triplicate in a 96-well plate in a final volume of 150 μl for 3 h at 37°C. Fluorescence was monitored by a fluorescence ELISA reader at excitation and emission wavelengths of 360 and 460 nm, respectively.

Heart perfusion

Hearts were perfused via the aorta as described before [12] in the absence or presence of different concentrations of HO-3538. After being washed (nonrecirculating period of 15 min), hearts were perfused under normoxic conditions for 10 min; the flow was subsequently discontinued for 30 min by inflating a balloon (ischemia), which was followed by 15 min of reperfusion. HO-3538 at the indicated concentrations was added at the beginning of the normoxic perfusion phase. Levels of high-energy phosphate intermediates were monitored in the magnet of a 31P NMR spectroscope during the entire perfusion.

NMR spectroscopy

NMR spectra were recorded with a Varian UNITYINOVA 400 WB instrument. 31P measurements (161.90 MHz) of perfused hearts were run at 37°C in a Z d SPEC 20-mm broadband probe (Nalorac Co., Martinez, CA, USA), applying WALTZ proton decoupling ($\gamma B2$ = 1.6 kHz) during the acquisition only. Field homogeneity was adjusted by following the 1H signal (w1/2 = 10–15 Hz). Spectra were collected with a time resolution of 3 min by accumulating 120 transients in each free induction decay. Flip-angle pulses of 45° were used after a 1.25-s recycle delay, and transients were acquired over a 10-kHz spectral width in 0.25 s, and the acquired data points (5000) were zero-filled to 16,384. Under the above conditions, relative concentrations of the species are proportional to the corresponding peak

areas, because interpulse delays exceeded four to five times the T1 values of the metabolites that were analyzed in the 31P experiments. Data were acquired from five independent experiments for each concentration of HO-3538.

Immunoblot analysis of perfused hearts

Myocardial specimens (n = 3 in each group) were snapfrozen immediately after surgical removal or at the end of the Langendorff-perfusion experiment and stored at −80°C until analyzed. Nuclear, mitochondrial and cytosolic fractions were prepared as described [33]. AIF, Endo G, and cyt-c were detected by immunoblotting from each fraction as described under "Detection of mitochondrial protein release." Experiments were repeated three times for each group and the results are illustrated by photomicrographs of representative blots.

Lipid peroxidation in perfused hearts

Lipid peroxidation was estimated from the formation of thiobarbituric acid reactive substances (TBARS). TBARS were determined using a modification of the method described previously [34]. Cardiac tissue was homogenized in 6.5% TCA and a reagent containing 15% TCA, 0.375% TBA, and 0.25% HCl was added, mixed thoroughly, heated for 15 min in a boiling water bath, cooled, and centrifuged and the absorbency of the supernatant was measured at 535 nm against a blank that contained all the reagents except the tissue homogenate. Using a malondialdehyde standard TBARS were calculated as nmol/g wet tissue.

Determination of infarct size in perfused hearts

For infarct size measurements, 90-min postischemic reperfusion was employed in hearts either untreated or treated with 5 μM HO-3538. After being removed from the Langendorff

perfusion apparatus, ventricles were cut off and kept overnight at −4°C. Frozen ventricles were sliced into 2- to 3-mm-thick sections and then incubated in 1% 2,3,54-triphenyl tetrazolium chloride (TTC) at 37°C in 0.2MTris buffer (pH 7.4) for 30 min. Whereas the normal myocardium was stained brick red, the infarcted areas remained unstained. Size of the infarcted area was estimated by the volume and weight method [32].

Statistical analysis

Data are presented as means ± SEM. For multiple comparisons of groups ANOVAwas used. Statistical difference between groups was established by paired or unpaired Student's t test, with Bonferroni correction.

Results.

Transdominant Expression of PARP-DBD in WRL-68 Liver Cell Line and Its Effect on the PARP Auto-ADP-ribosylation in Oxidative Stress

To achieve nonpharmacological competitive inhibition of the PARP-1 enzyme, we transiently transfected WRL-68 liver cells with constructs expressing the hybrid proteins consisting of a nuclear localization signal and the PARP-DBD attached either to the N (N3) or the C terminus (C1) of GFP (Fig. 8*A*). As expected, the C1 and N3 proteins were localized to the nucleus (Fig. 8, *B–D*), their electrophoretic mobility corresponded to the theoretical value calculated from the molecular weight of GFP and PARP-DBD (Fig. 8*E*), and they inhibited both the unstimulated and the oxidative stress-induced PARP activity (Fig. 9).

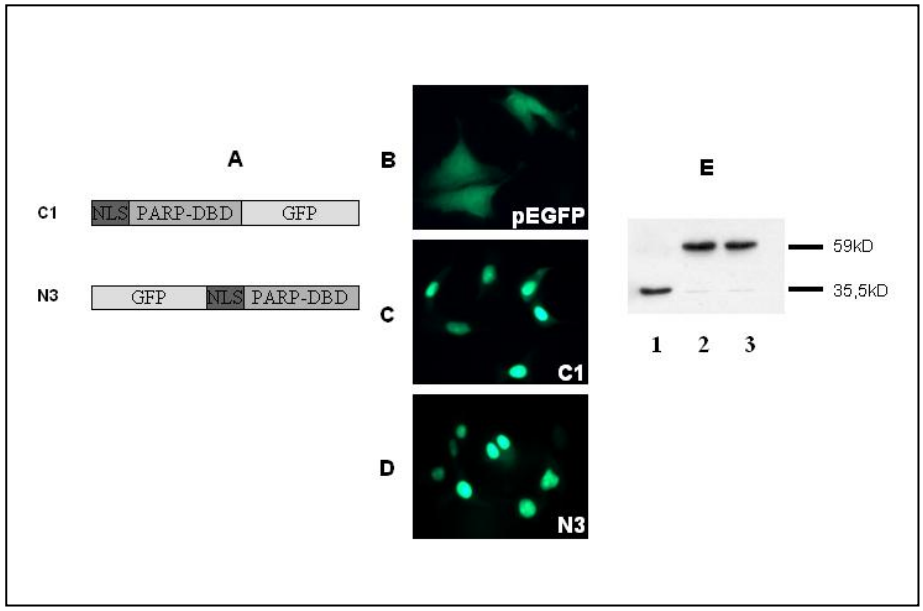

FIGURE 8. Transdominant expression of the PARP-DBD. *A, construction of PARP-DBD GFP fusion protein. WRL-68 liver cells were transfected with the pEGFP (B), C1pEGFP (C), or N3pEGFP (D) plasmids. GFP fluorescence was detected by fluorescent microscopy. Expression of the transfected proteins was detected by Western blotting utilizing anti-GFP antibody (E). Lane 1, cells transfected with pEGFP; lane 2, cells transfected with C1pEGFP; lane 3, cells transfected with N3pEGFP.*

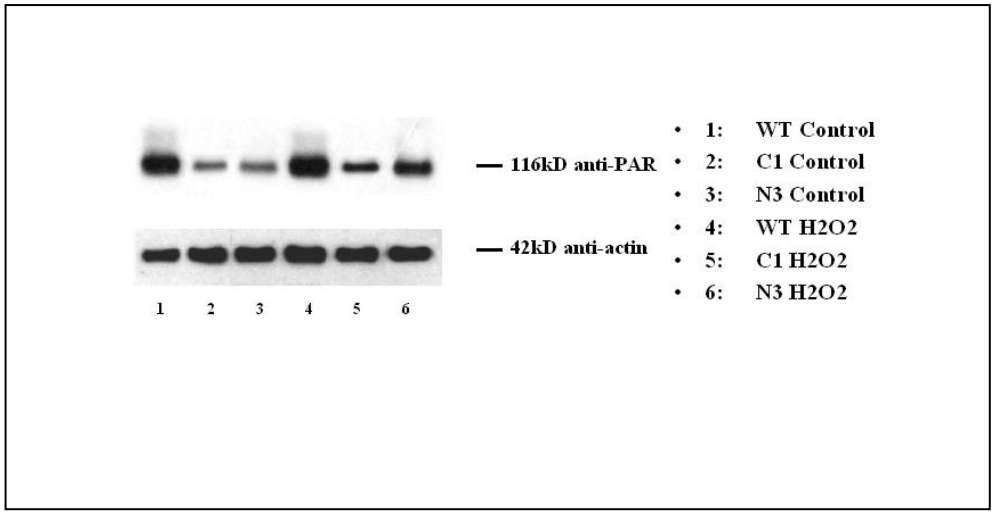

FIGURE 9. Effect of transdominant expression of PARP-DBD on the PARP auto-ADPribosylation in oxidative stress. *Wild type WRL-68 liver cells or cells transfected with pEGFP, C1pEGFP (C1), or N3pEGFP (N3) plasmids were treated with 1mM H2O2 for 1 h as indicated below. Auto-ADP-ribosylation of PARP in the cell homogenates was detected by Western blotting utilizing an anti-ADP-ribose antibody. Even protein loadings were confirmed by an anti-actin antibody and Western blotting. ADP-ribosylation in pEGFPtransfected cells was identical to that in untransfected cells either in the absence or the presence of H2O2 (data not shown). Lane 1, untransfected control cells; lane 2, C1 cells; lane 3,N3cells; lane 4, control cells_H2O2; lane 5,C1cells_H2O2; lane 6,N3cells_H2O2.*

Effect of Transdominant Expression of PARP-DBD on the Viability of WRL-68 Cells in Oxidative Stress

To evaluate the effect of the transdominant expression of PARP-DBD on the viability of human hepatocyte WRL-68 cells, we examined the direct cytotoxic effect of 0.3 mM H2O2 for 3 h (Fig. 10). The cell viability was detected by MTT assay and expressed as percent of the viability of untreated wild type cells. The transdominant expression of PARP-DBD protected WRL-68 cells from the H2O2-induced oxidative stress that proved to be significant (p <0.01). These results suggest that the enzymatic activity of nuclear PARP-1 is involved in the cytotoxicity of H2O2, and the inhibition of PARP-1 either by a pharmacological agent or by a nonpharmacological way protects against oxidative stress-related injuries.

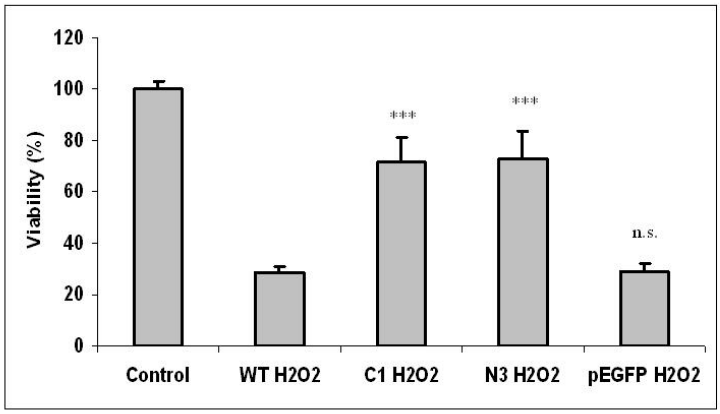

FIGURE 10. Effect of transdominant expression of PARP-DBD on the viability of WRL-68 cells in oxidative stress. *WRL-68 liver cells were transfected with pEGFP, C1, or N3 plasmids and were treated with 0.3mM H2O2 for 3 h. Cell viabilities were detected by MTT assay and were expressed as a percent of the untreated wild type cells (Control). Transfection by itself had no effect on the viability of cells (data not shown). ***, significantly different from H2O2-treated wild type (WT H2O2) p < 0.001 (n - 24); n.s., not different from WT H2O2.*

Comparison of the Effect of Transdominant Expression of PARP-DBD and of Pharmacological Inhibition of PARP on Akt Activation in Oxidative Stress

To establish the role of nuclear PARP-1 in regulating proteomic signal transduction pathways, we analyzed the activation of the Akt/protein kinase B pathway during oxidative stress in the presence of a well characterized PARP inhibitor; PJ-34, and the transdominant expression of PARP-DBD. WRL-68 liver cells transfected with pEGFP, C1, or N3 plasmids as well as wild type cells were treated with 1 mM H2O2 or with 1 mM H2O2 + 10 μM PJ-34 for 1 h as indicated. The transdominant expression of PARP-DBD (C1, N3) increased the phosphorylation of Akt (Ser473) during oxidative stress compared with wild type and caused an effect similar to that of the pharmacological inhibitor, PJ-34 (Fig. 11*A*). However, when the phosphorylation of Akt in transfected cells (C1, N3) was investigated under normal conditions without the induction of oxidative stress, its level was found to be

elevated compared with the wild type WRL-68 cells. Transfection by pEGFP plasmid had no effect on the phosphorylation of Akt (Ser473) (Fig. 11*B*). These results suggest that PARP-1 activity indeed can regulate Akt activation, and it can be a factor in the cytoprotective effect of PARP inhibition.

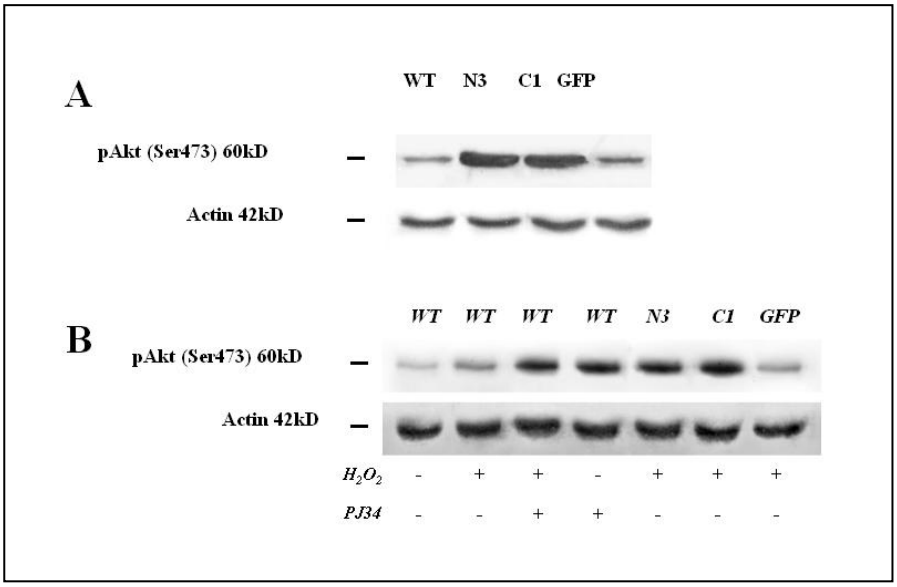

FIGURE 11. Comparison of the effect of pharmacological inhibition of PARP and of transdominant expression ofPARP-DBD on Akt activation in oxidative stress. *A, Akt activation in cells transfected with pEGFP, C1, or N3 plasmids as well as in wild type (WT) WRL-68 liver cells was demonstrated by Western blotting utilizing a phosphorylationspecific primary antibody (P-Ser473Akt). B, transfected and wild type cells were treated with 1 mM H2O2, 10 μM PJ-34 or with 1 mM H2O2 + 10 μM PJ-34 for 1 h as indicated. Akt activation in the cells was demonstrated as above. Even protein loadings were confirmed by an anti-actin antibody and Western blotting.*

Suppression of PARP by the siRNA Technique and Its Effect on the Viability of WRL-68 Cells in Oxidative Stress

WRL-68 liver cells were transfected with PARP-siRNA according to the manufacturer's recommendations. To reveal the efficiency of the silencing of PARP expression we compared the expression of the PARP gene of wild type cells with that of the PARP-siRNA transfected cells. Wild type and transfected cells were treated with 1mM H2O2 or 1 mM H2O2+10 μM PJ-34 for 1 h as indicated. PARP expression in the cell homogenates was

detected by Western blotting utilizing an anti-PARP antibody. The transfection of PARP-siRNA inhibited the PARP expression both under normal conditions as well as in oxidative stress (Fig. 12). We investigated the effect of the suppression of PARP by the siRNA technique on the viability of WRL-68 cells in oxidative stress. WRL-68 liver cells transfected with PARP-siRNA as well as wild type cells were treated with 0, 0.3, 1, or 3 mM H2O2 for 3 h. Cell viabilities were detected by MTT assay and were expressed as a percent of the viabilities of untreated wild type cells (Fig. 13). Suppression of PARP by the siRNA technique decreased the H2O2- induced injuries in all cases.

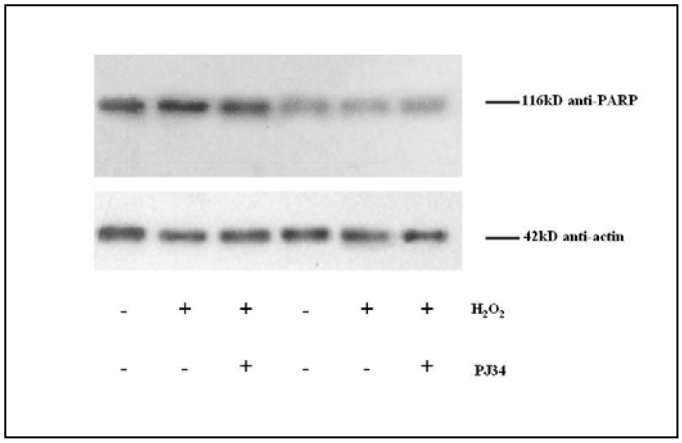

FIGURE 12. Suppression of PARP by the siRNA technique. *WRL-68 liver cells were transfected with PARP-siRNA according to the manufacturer's recommendations. Wild type and transfected cells were treated with 1mM H2O2or1mM H2O2+10 μM PJ-34 for 1 h as indicated. PARP expression in the cell homogenates was detected by Western blotting utilizing an anti-PARP antibody. Even protein loadings were confirmed by an anti-actin antibody and Western blotting. Left three lanes, untransfected cells; right three lanes, cells transfected with PARP-siRNA.*

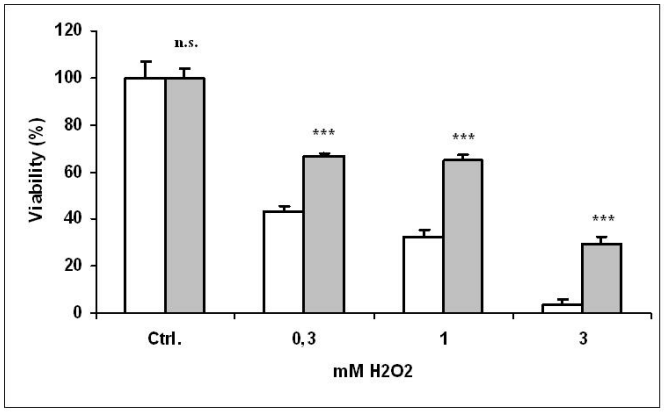

FIGURE 13. Effect of PARP-suppression on the viability of WRL-68 cells in oxidative stress. *WRL-68 liver cells transfected with PARP-siRNA (filled bars) as well as wild type cells (open bars) were treated with 0, 0.3, 1, or 3 mM H2O2 for 3 h. Cell viabilities were detected by MTT assay and were expressed as a percent of the untreated wild type cells. ***, significantly different from the wild type cells of same H2O2 treatment, p<0.001 (n-24); n.s., not different from wild type.*

Comparison of the Effect of Pharmacological Inhibition of PARP and of Its Suppression by siRNA on Akt Activation in Oxidative Stress

WRL-68 liver cells transfected with PARP-siRNA as well as wild type cells were treated with 1 mM H2O2 or with 1 mM H2O2 + 10 μM PJ-34 for 1 h as indicated. Akt activation in the cells was demonstrated by Western blotting utilizing a phosphorylation-specific primary antibody (P-Ser473Akt). Both the pharmacological inhibition (PJ-34) and the suppression of PARP by siRNA affected phosphorylation of Akt (Ser473) the same way compared with wild type cells in the presence or absence of H2O2 (Fig. 14). These results fully supported those we acquired with the transdominant expression of PARP-DBD.

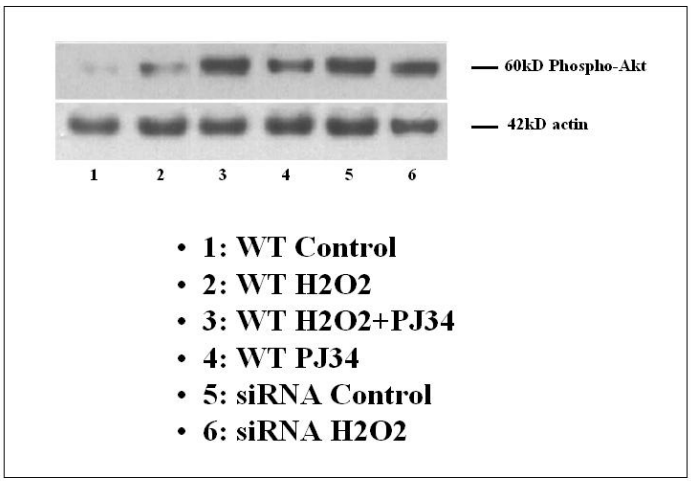

FIGURE 14. Comparison of the effect of pharmacological inhibition of PARP and of its suppression by siRNA on Akt activation in oxidative stress. *WRL-68 liver cells transfected with PARP-siRNA as well as wild type (WT) cells were treated with 1 mM H2O2 or with 1 mM H2O2 µ10 µM PJ-34 for 1 h as indicated. Akt activation in the cells was demonstrated by Western blotting utilizing a phosphorylation-specific primary antibody (P-Ser473Akt). Even protein loadings were confirmed by an anti-actin antibody and Western blotting.*

Effect of PARP Inhibition and Kinase Inhibitors on the Viability and NAD$^+$ Content of WRL-68 Cells in Oxidative Stress

To establish further the role of the Akt pathway among the molecular mechanisms in the protective effect of PARP inhibition in H2O2-induced oxidative stress, we analyzed the effect of a specific PI3-kinase inhibitor, LY 294002, and an Src kinase inhibitor, Pp2 on the viability and NAD-content of WRL-68 liver cells. The cells were treated for 3 h with 0.3mM H2O2, 10 µM PJ-34, 10 µM LY 294002, or 10 µM Pp2, or with different combinations of these compounds as indicated. Cell viabilities were detected by MTTassay and were expressed as a percent of the untreated cells. PJ-34 significantly ($p < 0.001$) decreased the toxicity of H2O2 in WRL-68 cells. However, when LY 294002 at a concentration of 10 µM was also present, the protective effect of PJ-34 was significantly ($p < 0.001$) diminished (Fig. 15*A*). Similar results were obtained in the presence of 1 µM wortmannin (data not shown). The specific inhibitor of Src kinase; Pp2, at a concentration

of 10 μM, significantly decreased the protective effect of PJ-34 on theH2O2-induced oxidative stress (Fig. 15*A*), the same way as the PI3-kinase inhibitors did. The specific PI3-kinase inhibitor LY 294002 and the Src kinase inhibitor diminished the protective effect of both the transdominant expression of PARP-DBD and suppression of PARP by siRNA compared with the pEGFP plasmidtransfected cells that were used as a negative control (Fig. 15*B*). When added alone to the cells, PJ-34, LY 294002, and Pp2 did not affect the viability of the cells. To compare the significance of Akt activation with that of prevention of NAD^+ depletion among the mechanisms of the cytoprotective effect of PARP inhibition, we determined the NAD^+ content of the cells treated identically to those used for viability measurements. We found that the 3-h treatment with 0,3 mM H2O2 induced about an 80% drop in the cellular NAD^+ content of both unprotected WRL-68 cells and the cells transfected with the pEGFP plasmid (Fig. 16). PJ-34 treatment, transdominant expression of the PARP-DBD, or suppression of PARP by siRNA partially, although significantly ($p < 0.05$ and $p < 0.001$) diminished this NAD- depletion, resulting in levels of about 50% that of untreated cells (Fig. 14). In contrast to the cell viability measurements, the PI3-kinase and Src kinase inhibitors did not interfere with the protective effect of PARP inhibition (Fig. 14). PARP inhibition or the PI3-kinase and Src kinase inhibitors did not affect the cellular NAD^+ levels in the absence of oxidative stress (Fig. 14). These data suggest that the diminishing of NAD^+ depletion alone could not account for the cytoprotective effect of PARP-1 inhibition, and the activation of the Akt/ protein kinase B pathway should indeed be involved in the molecular mechanisms of it.

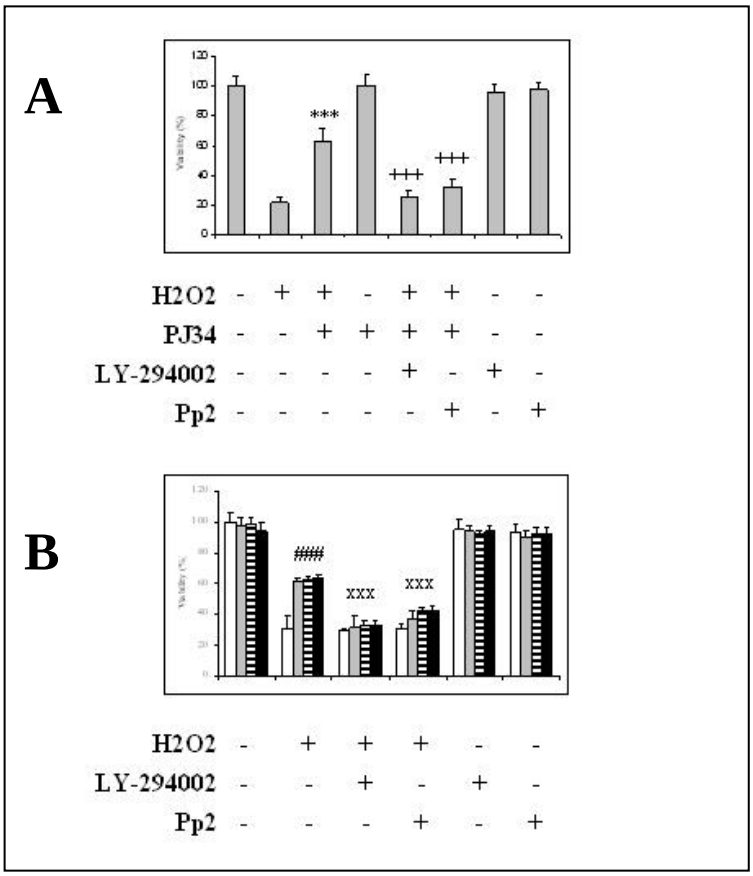

FIGURE 15. Effect of PARPinhibition and different kinase inhibitors on the viability of WRL-68 cells in oxidative stress. *A, WRL-68 liver cells were treated for 3 h with 0.3 mM H2O2, 10 μM PJ-34, 10 μM LY 294002, or 10 μM Pp2, or with different combinations of these compounds as indicated. Cell viabilities were detected by MTT assay and were expressed as a percent of the untreated cells. B, WRL-68 liver cells were transfected with pEGFP (open bars), C1 (gray filled bars), N3 plasmids (horizontal striped bars), or PARPsiRNA (black filled bars) and were treated for 3 h with 0.3mMH2O2, 10 μM LY 294002, or 10 μM Pp2, or with different combinations of these compounds as indicated. Cell viabilities were detected by MTT assay and were expressed as a percent of the untreated cells. ***, significantly different from H2O2-treated cells, p < 0.001 (n - 24); +++, significantly different from H2O2+PJ-34-treated cells, p<0.001 (n-24); ###, significantly different from pEGFP-transfected cells, p<0.001 (n-8); xxx, significantly different from cells not treated with Pp2 and LY 294002, p < 0.001 (n - 8).*

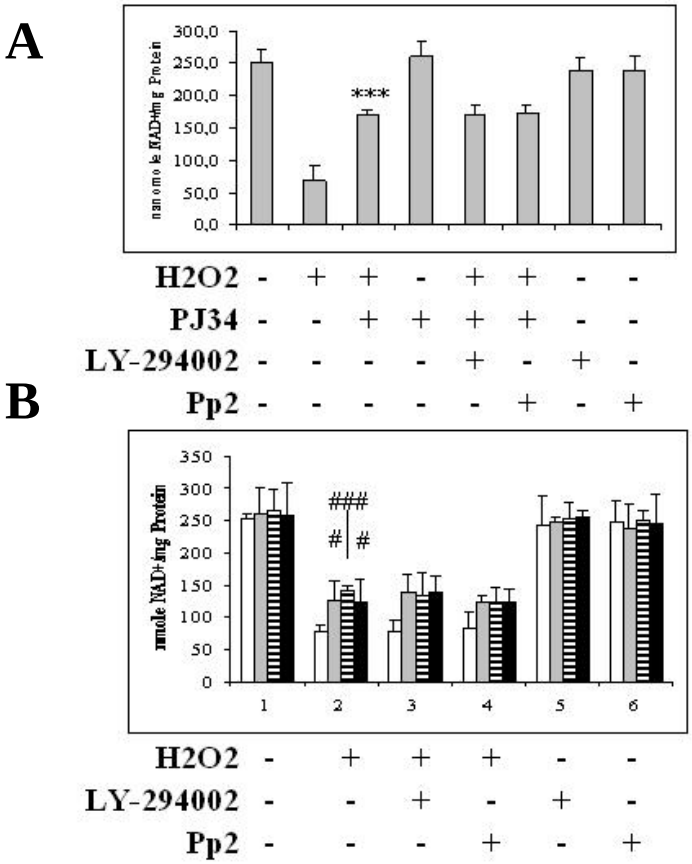

FIGURE 16. Effect of PARP inhibition and different kinase inhibitors on the NAD-content of WRL-68 cells in oxidative stress. *A, WRL-68 liver cells were treated for 3 h with 0.3mM H2O2, 10 μM PJ-34, 10 μM LY 294002, or 10 μM Pp2, or with different combinations of these compounds as indicated. Cellular NAD^+ levels were determined and expressed as nmol of NAD^+/mg of protein. B, WRL-68 liver cells were transfected with pEGFP (open bars), C1 (gray filled bars), N3 plasmids (horizontal striped bars), or PARPsiRNA (black filled bars) and were treated for 3 h with 0.3mMH2O2, 10 μM LY 294002, or 10 μM Pp2, or with different combinations of these compounds as indicated. Cellular NAD^+ levels were determined and expressed as nmol of NAD^+/mg of protein. ***, significantly different from H2O2-treated cells, $p < 0.001$ (n - 12); #, significantly different from pEGFP-transfected cells, $p < 0.05$ (n - 8); ###, significantly different from pEGFP-transfected cells, $p<0.001$ (n - 8).*

Effect of the PI3-Kinase and Src Kinase Inhibitors on the Oxidative Stress- and PARP Inhibition-induced Akt Pathway Activation

To confirm the previous conclusion, we analyzed the effect of PI3-kinase and Src kinase inhibitors in combination with that of PARP inhibition on oxidative stress-induced activation of Akt/protein kinase B and the phosphorylation of its downstream target GSK3β. The experimental setup was similar to that used for the viability and NAD^+

measurements. Wild type WRL-68 cells were treated for 1 h with1mMH2O2, 10 μM PJ-34, 10 μM LY 294002, or 10 μM Pp2, or with different combinations of these compounds as indicated in Fig. 15. Both LY 294002 and Pp2 decreased the PJ-34-induced Akt or GSK3 β phosphorylation during oxidative stress (Fig. 17*A*) as did 1 μM wortmannin (data not shown). When added alone to the cells, LY 294002, wortmannin, and Pp2 gave results identical to those of untreated cells (data not shown). When the expression of PARP enzyme was blocked by PARP-siRNA in WRL-68 cells, or the cells were transfected with C1 or N3 plasmids, we observed the same effect as in the case of the pharmacological inhibitor PJ-34 during oxidative stress. Akt and its downstream target GSK3 β were phosphorylated, and this effect was diminished because of the specific PI3-kinase inhibitor LY 294002 or Src kinase inhibitor Pp2. Transfection by pEGFP plasmid had no effect on the phosphorylation of Akt (Ser473) or GSK3 β (Fig. 17*B*).

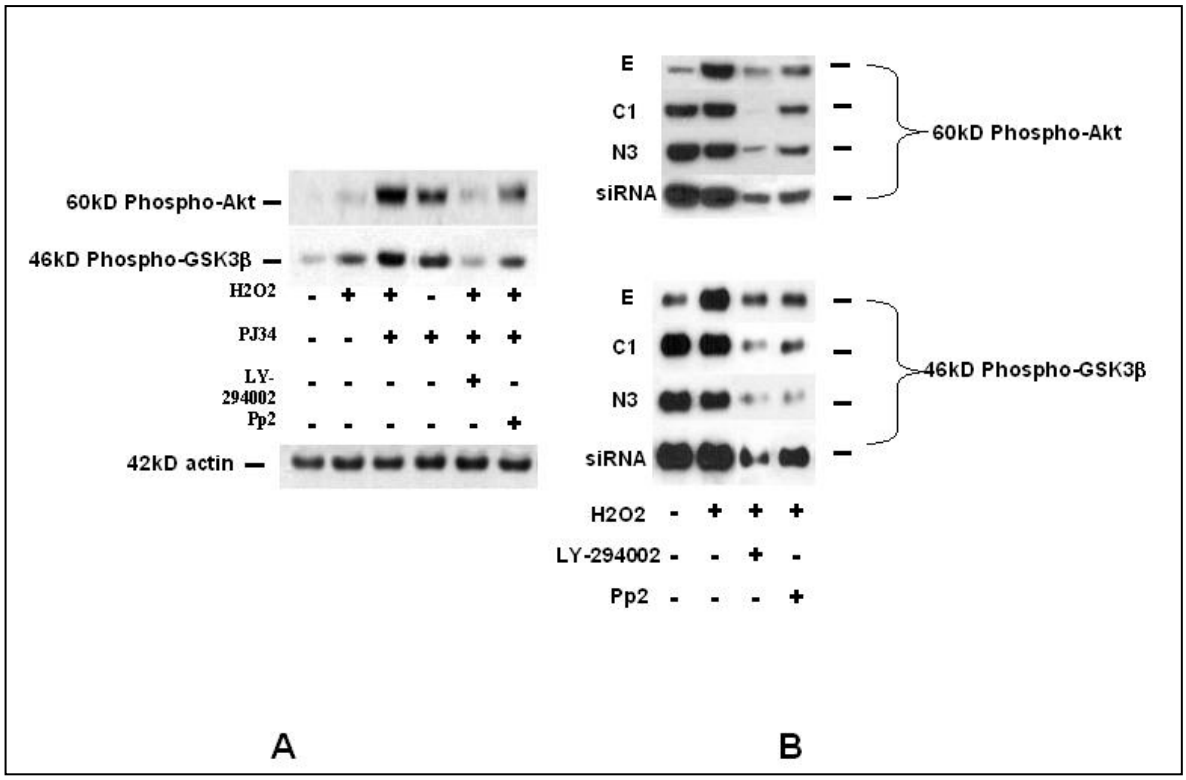

FIGURE 17. Modulation of the activation of Akt pathway by oxidative stress, PARP inhibition, and different kinase inhibitors. *Activation of Akt and phosphorylation of its downstream target GSK3β were studied in WRL-68 liver cells by Western blotting utilizing phosphorylation-specific primary antibodies (P-Ser473Akt and P-Ser9GSK3β, respectively). A, the wild type WRL-68 cells were treated for 1 h with1mM H2O2, 10 μM PJ-34, 10 μM LY 294002, or 10 μM Pp2, or with different combinations of these compounds as indicated. B, WRL-68 liver cells were transfected with PARP-siRNA or pEGFP, C1, or N3 plasmids and were treated for 1 h with 1 mM H2O2, 10 μM LY 294002, or 10 μM Pp2, or with different combinations of these compounds as indicated. When added alone to the cells, LY 294002 and Pp2 gave results identical to those of untreated cells for both antibodies (data not shown). Even protein loadings were confirmed by an anti-actin antibody and Western blotting.*

Effect of PARP Inhibition, Kinase Inhibitors, PARP Suppression, and Transdominant Expression of PARP-DBD on the Mitochondrial Membrane Potential of WRL-68 Cells in Oxidative Stress

We investigated the effect of the suppression of PARP by PARP-siRNA and PARP inhibition by transdominant expression of PARP-DBD as well as by PJ-34 on the mitochondrial membrane potential of WRL-68 cells utilizing a specific, mitochondrial

membrane potential-dependent fluorescent dye; JC-1. WRL-68 liver cells as well as pEGFP, C1, N3 plasmid, or PARPsiRNA- transfected cells were treated for 3 h with 0.3 mM H2O2, 10 μM PJ-34, 10 μM LY 294002, or 10 μM Pp2. After the treatment, cells were loaded with JC-1, and fluorescence images were acquired in the green and red channels of the microscope. Images of healthy cells with intact undamaged mitochondria were sharp and rich in both red and green components appearing on the merged image as yellow (Fig. 18*A*, *first picture*). However, cells with damaged mitochondria showed characteristically different images; they appeared blurred and completely lacking red components because of the loss of mitochondrial membrane potential (Fig. 18*A*, *second picture*). The pharmacological inhibitor PJ-34 protected the mitochondrial membrane potential from the H2O2-induced injury, and the specific kinase inhibitors LY 294002 or Pp2 counteracted the protection of PJ-34 (Fig. 18*A*) as did wortmannin (data not shown). The C1 or N3 plasmid-transfected cells exerted a greater resistance against H2O2-induced injury compared with the wild type WRL-68 cells, and this protective effect was decreased by the specific kinase inhibitor; LY 294002, Pp2, or wortmannin. Transfection by pEGFP plasmid could not influence the mitochondrial membrane potential of the WRL-68 cells (Fig. 18*B*). The suppression of PARP by the siRNA technique had an effect on the mitochondrial membrane potential of WRL-68 cells identical to that of the transdominant expression of PARP-DBD, and the resistance of the PARP-siRNA-transfected cells against H2O2-induced oxidative stress could also be decreased by the specific kinase inhibitors, LY 294002 or Pp2 (Fig. 18*C*).

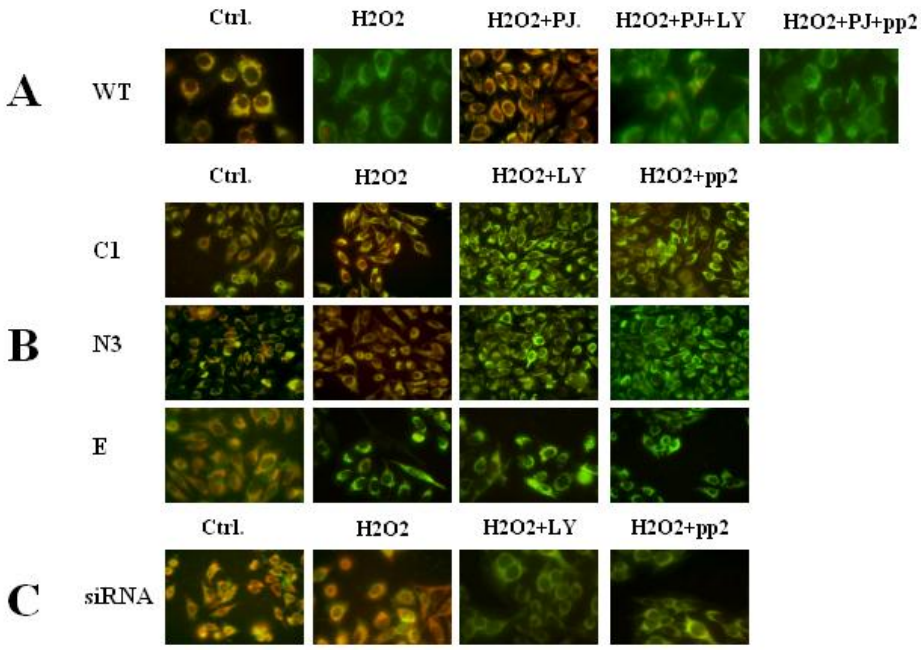

FIGURE 18. Effect of PARP inhibition, different kinase inhibitors, PARP suppression, and transdominant expression of PARP-DBD on the mitochondrial membrane potential of WRL-68 cells in oxidative stress. *Green and red fluorescence images were merged and used to demonstrate the effect of the following treatments on the mitochondrial membrane potential of WRL-68 liver cells. A, WRL-68 liver cells were treated for 3 h with 0.3mMH2O2, 10 μM PJ-34, 10 μM LY 294002, or 10 μM Pp2. B, WRL-68 liver cells were transfected with pEGFP, C1, or N3 plasmid and were treated for 3 h with 0.3mM H2O2, 10 μM LY 294002 or 10 μM Pp2, or with different combinations of these compounds as indicated. C, WRL-68 liver cells were transfected with PARP-siRNA and treated for 3 h with 0.3mM H2O2, 10 μM LY 294002, or 10 μM Pp2, or with different combinations of these compounds as indicated. After the treatment, the medium was replaced with fresh medium without any agents and containing 1 μM JC-1 membrane potential-sensitive fluorescent dye. After 10-min loading, digital images were acquired using a fluorescent microscope equipped with a digital camera.*

Effect of HO-3538 on the mitochondrial permeability transition

In order to further characterize the role of mitochondrial events in cytoprotection, we studied the effect of HO-3538, a novel mitochondrial permeability transition inhibitor with free-radical scavenger activity, on swelling of isolated mitochondria. High-amplitude swelling of the mitochondria due to permeability transition was monitored by the decrease

of reflectance of 540 nm light. In Percoll gradient purified rat liver mitochondria, the swelling induced by 150 μM of Ca^{2+} (Fig 19A, line 2) was completely inhibited by 2.5 μM of cyclosporine A (Fig. 19A, line 3). HO-3538 inhibited the mitochondrial swelling induced by Ca^{2+} in a concentration dependent manner with the IC_{50} of 4.9 ± 0.5 μM (Fig. 19A, lines 4-7). The effect of HO-3538 on isolated rat heart mitochondria was basically the same (Fig 19B, lines 4-7). HO-3538 completely inhibited the Ca^{2+}-induced swelling above the concentration of 40 μM, as did 2.5 μM of cyclosporine A. HO-3538 did not induce swelling on its own up to the concentration of 100 μM in isolated rat liver (Fig. 19C, lines 3-7) or isolated rat heart mitochondria (Fig. 19D, lines 3-7). Similar inhibitory effects by HO-3538 were observed when the mitochondrial swelling was induced by other agents such as *tert*-butyl hydroperoxide or atractyloside (data not shown). The free-radical scavenging side-chain of HO-3538 did not have any effect on the calcium induced mitochondrial swelling up to the concentration of 100 μM (data not shown).

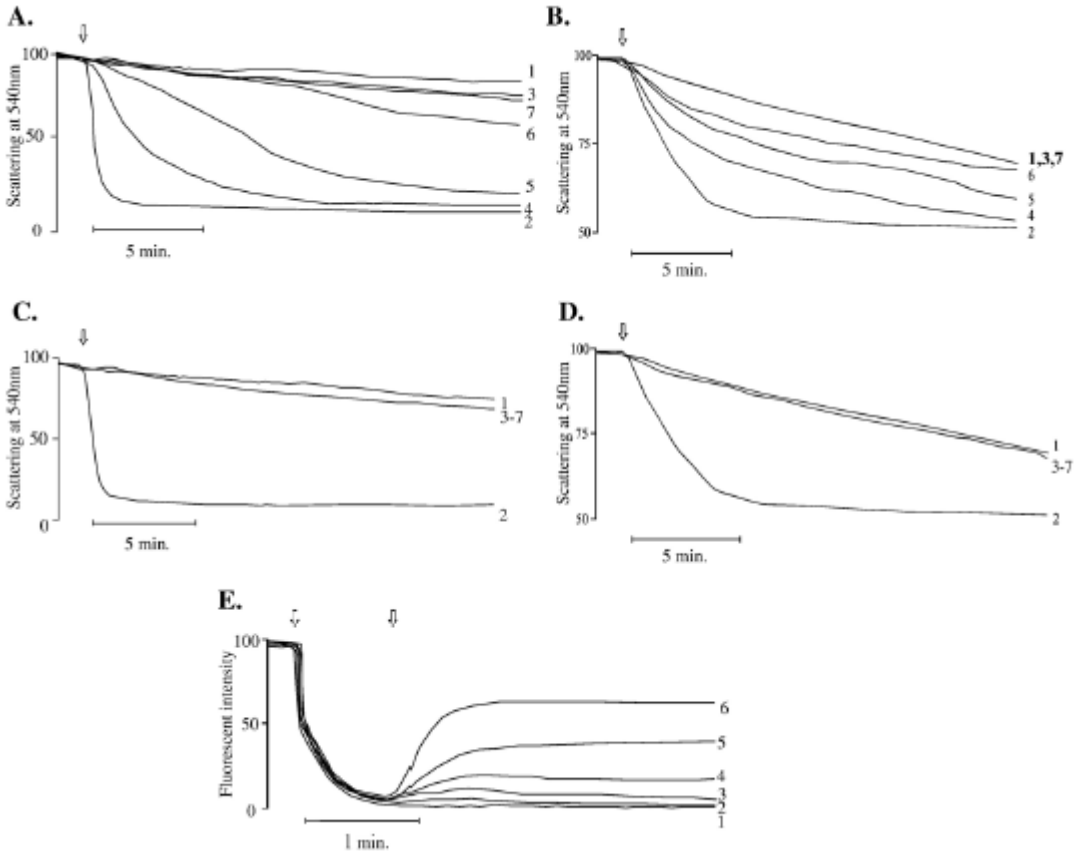

Fig. 19. Direct effects of HO-3538 on isolated mitochondria.
Mitochondrial swelling was demonstrated by monitoring E_{540} in isolated rat liver mitochondria. HO-3538 at the indicated concentration or 2.5 µM cyclosporin A (CsA) was present throughout the experiment. The mitochondrial permeability transition (swelling) was induced in isolated rat liver (A) or heart (B) mitochondria by adding 150 µM Ca^{2+} indicated by the arrow. Line 1: baseline swelling (no agent); line 2: 150 µM $Ca2^{+}$- induced swelling ; line 3: 150 µM $Ca2^{+}$ + 2.5 µM CsA; line 4: 5 µM HO-3538; line 5: 10 µM HO-3538; line 6: 20 µM HO-3538; and line 7: 50 µM HO-3538. The mitochondrial permeability transition (swelling) was induced by adding 150 µM Ca^{2+} or attempted by different concentrations of HO-3538 in isolated rat liver (C) or heart (D) mitochondria, indicated by the arrow. Line 1: baseline swelling (no agent); line 2: 150 µM $Ca2^{+}$-induced swelling; line 3: 5 µM HO-3538; line 4: 10 µM HO-3538; line 5: 20 µM HO-3538;line 6: 50 µM HO-3538; and line 7: 100 µM HO-3538. (E). Membrane potential was monitored by measuring the fluorescent intensity of the cationic fluorescent dye rhodamine 123. Isolated heart mitochondria, added at the first arrow, takes up the dye in a voltage dependent manner and quenches its fluorescence. HO-3538 at the concentrations indicated or 150 µM Ca^{2+} (either added at second arrow) induces depolarization resulting in release of the dye and increase of the fluorescence intensity. Line 1, no agent; line 2, 5 µM HO-3538; line 3, 10 µM HO-3538; line 4, 20 µM HO-3538; line 5, 50 µM HO-3538; line 6, 150 µM $Ca2^{+}$.

Effect of HO-3538 on the mitochondrial membrane potential (Δψ)

150 μM of Ca^{2+} induced the decrease of the ΔΨ as detected by the release of the membrane potential sensitive dye, Rh123 from isolated heart mitochondria (data not shown). HO-3538 also caused a concentration dependent dissipation of ΔΨ (Fig. 19E) with an EC_{50} value of 36.2 ± 3.2 μM. The effect of HO-3538 on the membrane potential of liver mitochondria was basically the same (data not shown). Since the uncoupling effect, that is dissipation of ΔΨ by HO-3538 was found to be negligible up to the concentration of 10 μM while it simultaneously exerted a strong inhibitory effect of the mPT at this concentration range, we used HO-3538 at the concentration of 10 μM for the further studies in isolated mitochondria.

Effect of HO-3538 on the release of pro-apoptotic protein from isolated heart mitochondria

The pro-apoptotic proteins AIF, Endo G and cyt-c, are sequestered within the mitochondria, and are released following an apoptotic or necrotic stimuli. Mitochondrial permeability transition was induced in isolated rat heart mitochondria by 150 μM of Ca^{2+} as described above causing the release of AIF, Endo G and cyt-c from the mitochondria (pellet, P) into the buffer (supernatant, S). This release of pro-apoptotic proteins was inhibited by 2.5 μM of cyclosporine A. HO-3538, alone at the concentration of 10 μM did not have any effect on the release of the mitochondrial proteins (data not shown). However, when the mitochondrial swelling was induced by 150 μM of Ca^{2+}, 10 μM of HO-3538 inhibited the release of AIF, Endo G and cyt-c, with an effect comparable to cyclosporine A and somewhat stronger than that of equimolar amiodarone (Fig. 20). Inhibitory effect of HO-3538 on the Ca^{2+} induced cytochrome c release was quantified by using an HPLC method. According to our results, cyclosporine A, HO-3538 and amiodarone inhibited the

cytochrome c release by 92.1 ± 2.5% ($p<0.005$), 81.4 ± 4.5% ($p<0.005$) and 72.5 ± 5.2% ($p<0.05$), respectively.

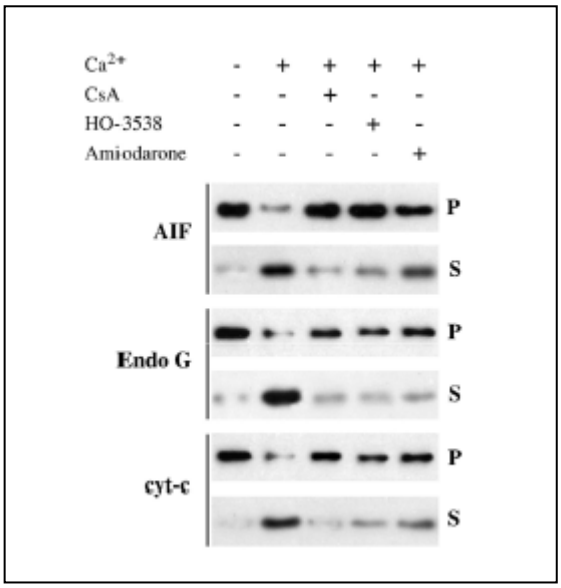

Fig. 20. Effect of HO-3538 on the release of pro-apoptotic mitochondrial proteins from isolated rat heart mitochondria. *AIF, EndoG and cyt-c were detected from the pellet (P) as unreleased or from the supernatant (S) as released pro-aportotic mitochondrial proteins by immunoblot analysis. The mitochondrial permeability transition was induced by 150 μM Ca^{2+} in the absence or presence of 2.5 μM of CsA or 10 μM of HO-3538. Lane 1: control (no agent added); lane 2: 150 μM of Ca^{2+}; lane 3: 150 μM of Ca^{2+} + 2.5 μM of CsA; lane 4: 150 μM of Ca^{2+} + 10 μM of HO-3538. The photomicrographs demonstrate representative blots of five independent experiments.*

Effect of HO-3538 on the viability of cardiomyocytes

On isolated mitochondria, we found considerable difference between amiodarone and HO-3538 in respect to their mPT inducing effect at higher concentrations. We investigated whether this difference manifested in any effect on cell viability. To this end we administered different concentrations of HO-3538 or amiodarone to H9C2 cardiomyocytes for 48 hours. Our results show that unlike amiodarone, HO-3538 did not affect the viability of the cardiomyocytes up to the concentration of 100 μM as detected by the MTT^{+} method (Fig. 21A). Amiodarone at the concentrations of 30 μM or 100 μM significantly decreased the viability of H9C2 cells when compared to equimolar amounts of HO-3538 (Fig. 21A).

To reveal any cytoprotective effect of HO-3538 in H9C2 cell line, we administered H_2O_2 in the presence of 10 μM amiodarone, HO-3538, SCAV, Vitamine E, Vitamine C and N-acetyl cysteine for 24 hours, then the cell viability was assessed by the MTT^+ method. The results demonstrate that the 150 μM of H_2O_2 caused a substancial cell death. Among the substances tested, cytoprotective effect of HO-3538 was significantly the most effective (Fig. 21B).

Effect of HO-3538 on the caspase-3 activation in cells

To assess the presumed anti-apoptotic effect of HO-3538 at cellular level, we induced apoptosis in Jurkat cells by administering 50 μM of etoposide for 12 hours, and detected caspase-3 activation (DEVD-ase). HO-3538 significantly decreased the DEVD-ase activity induced by etoposide (Fig. 21C) at the concentration of 5 μM or 10 μM ($p<0.05$ or $p<0.01$, respectively). When administered at higher concentrations, HO-3538 did not decrease any further the DEVD-ase activity induced by etoposide (data not shown). SCAV did not affect caspase-3 activity either in the presence or absence of etoposide, and HO-3538 did not induce it either in the absence of etoposide (data not shown).

ROS scavenging effect of HO-3538 in cardiomyocytes

In vivo ROS scavenger effect of HO-3538 was compared to that of some well established antioxidant compounds as well as of SCAV and amiodarone. In order to avoid any direct interaction with exogeniously added ROS in the medium, the H_2O_2 used for inducing ROS formation in H9C2 cells was removed before introducing HO-3538 or the other agents used at equimolar concentrations to the incubation medium. ROS levels in the cells were quantified by measuring the fluorescence of carboxy-DCFDA oxidized stochiometrically by the ROS from non-fluorescent carboxy-H_2DCFDA added to the medium 30 min after the other agents. All the agents tested significantly diminished the H_2O_2-induced ROS

formation in the H9C2 cardiomyoblasts. However, amiodarone was significantly less efective while SCAV and Vitamin C were more effective than HO-3538 (Fig. 21D).

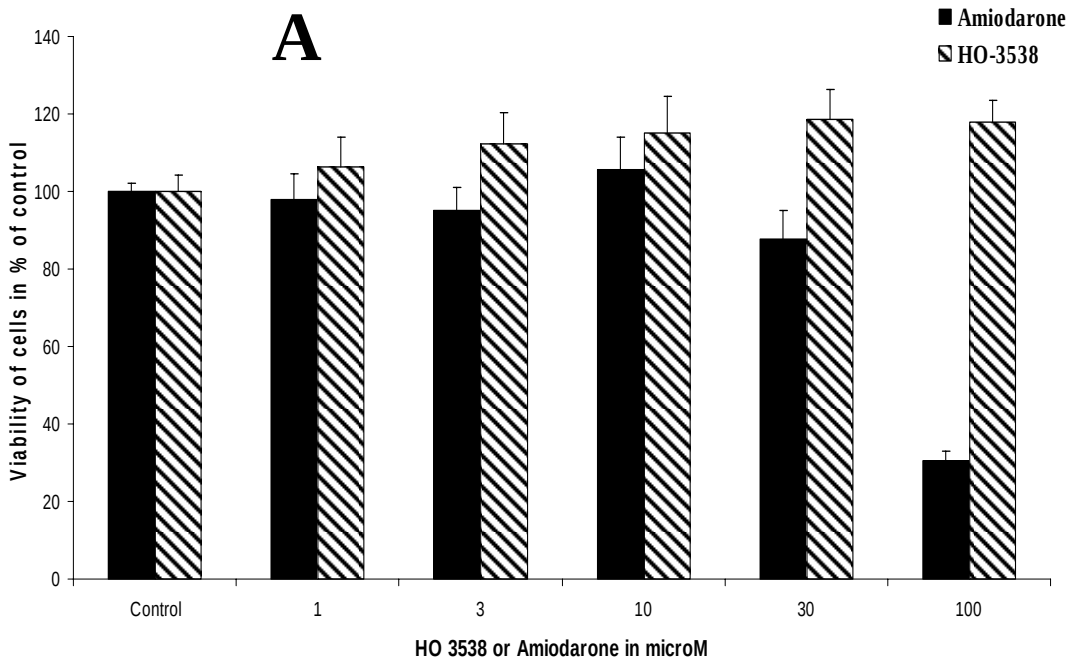

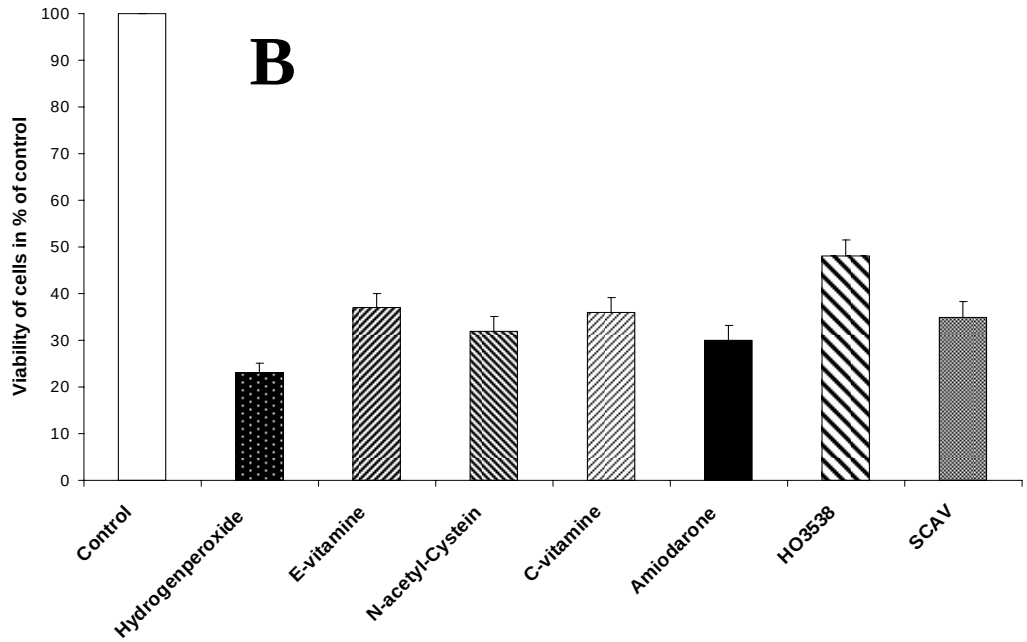

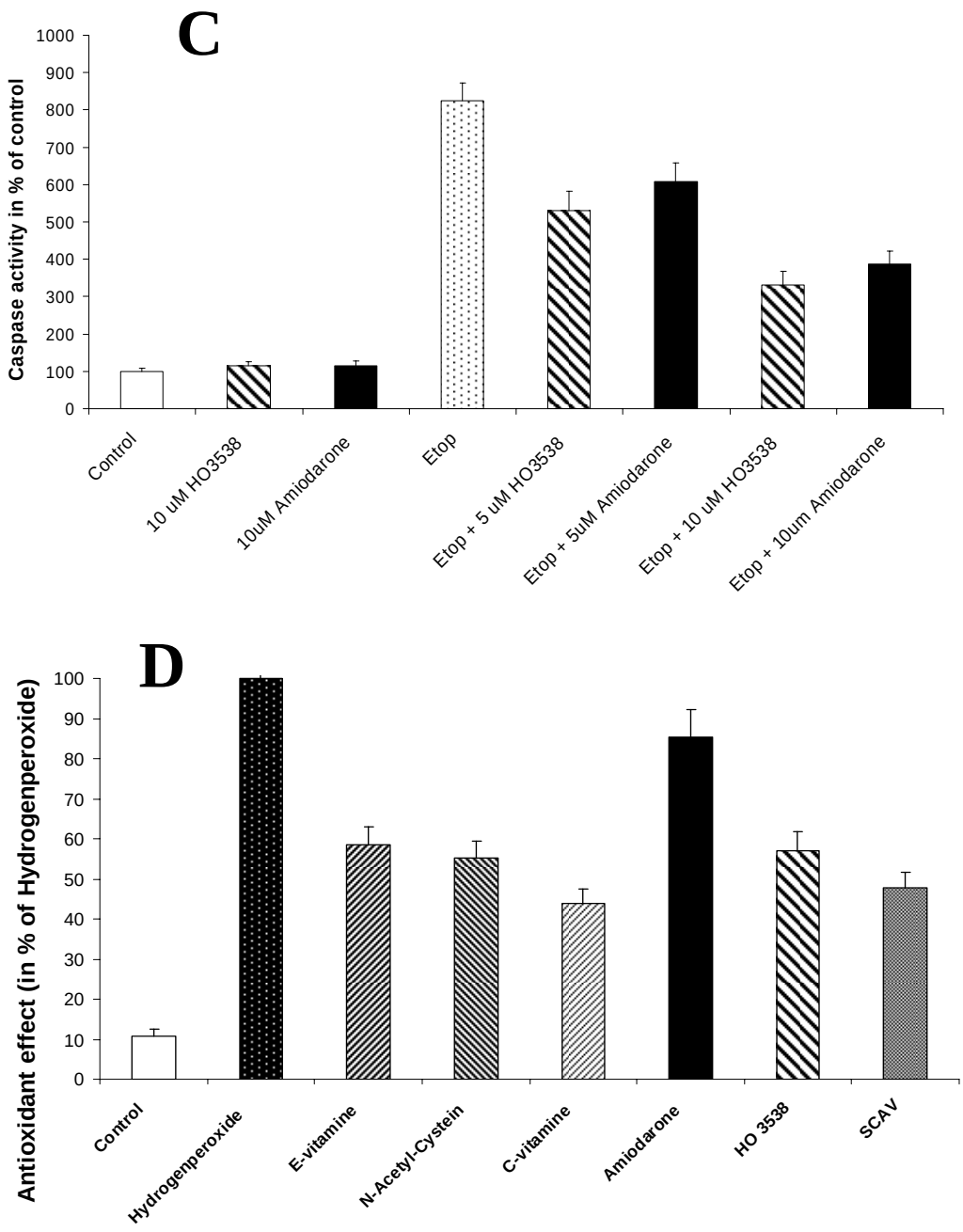

FIGURE 21. Toxicity and cytoprotective effect of amiodarone and HO-3538 in cardiomyblasts. *(A) The effect of amiodarone (filled columns) and HO3538 (diagonally striped columns) on the viability of H9C2 cardiomyoblasts as detected by the formation of water-insoluble blue formasan dye from the yellow mitochonrial dye MTT^+. The cells were exposed to different concentrations of amiodarone or HO-3538 for 48 h before the addition of the MTT^+ dye.*
(B) The effect of different compounds on the viability of H9C2 cells as detected by MTT^+. The cells were exposed to 150 μM of H_2O_2 for 24 h in the presence of 10 μM concentration of the different compounds tested (indicated underneath the column). Open column represent the control (no agent added), to which the viabilities were normalised (100%). Data represents average ± S.E.M of three independent experiment running in four parallels.

(C) Anti-apoptotic effect of HO-3538 and amiodarone. Apoptosis was induced in Jurkat cells by administering 50 μM of etoposide (Etop) for 12 hours in the absence or presence of amiodarone and HO-3538, and the activity of caspase-3 was detected by the fluorescent caspase-3 substrate, Ac-DEVD-AMC. Open column represent the control (no agent added). Data represents average ± S.E.M of three independent experiment running in three parallels.
(D) ROS scavenging effect of different compounds in H9C2 cells. To induce ROS formation, the cells were exposed to 1 mM of H_2O_2 for 90 min, then the medium was replaced to fresh one containing 10 μM of the different compounds tested (indicated underneath the column). After 30 min of incubation non-fluorescent carboxy-H_2DCFDA was added to the medium for an other hour of incubation. Fluorescence of carboxy-DCFDA oxidised by the ROS was detected by a fluorescent ELISA reader and was normalised to the H_2O_2 only value. Open column represent the control (no agent added). Data represent mean ± S.E.M. of three experiments running in four parallels.
*Significantly different from HO-3538: *, $p < 0.05$; **, $p < 0.01$); ***, $p < 0.001$*

Effect of HO-3538 on the mitochondrial protein release following ischemia-reperfusion in Langendorff-perfused hearts

We determined mitochondrial release of AIF, Endo G and cyt-c by using immunoblotting after subcellular fractionation of hearts that underwent the perfusion experiment. Ischemia-reperfusion induced the release of pro-apoptotic proteins from the mitochondria and caused nuclear translocation of AIF and Endo G. As it is demonstrated on Fig. 22, HO-3538 prevented this release as revealed by the retainment of the proteins in the mitochondrial fraction and their diminished presence in the nuclear or cytosolic fractions. Amiodarone and SCAV inhibited the release of pro-apoptotic proteins less effectively than HO-3538. Amount of cyt-c in the cytosolic fraction was quantified by HPLC technique, and it was found that HO-3538, amiodarone and SCAV reduced the ischemia-reperfusion induced cyt-c release by 70.3 ± 5.5, 61.7 ± 3.8 ($p<0.05$) and 44.4 ± 3.5 % ($p<0.001$), respectively

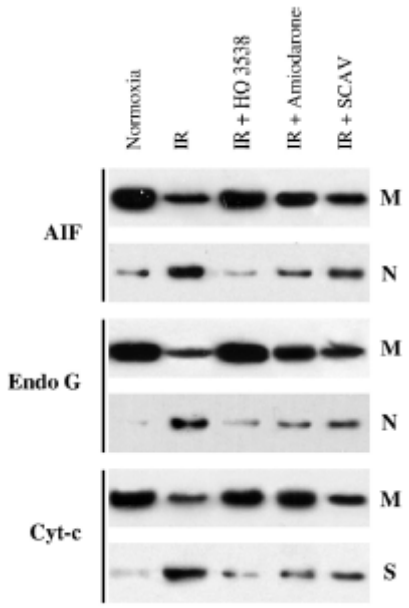

Fig. 22. Effect of HO3538 on the release of pro-apoptotic mitochondrial proteins following ischemia-reperfusion in Langendorff-perfused hearts. *The hearts were exposed to 30 min of ischemia followed by 15 of reperfusion, then they were subjected to subcellular fractionation. AIF, EndoG and cyt-c were detected from the mitochondrial fraction (M) as unreleased and from the nuclear (N) or the cytosolic (S) fraction as released pro-aportotic mitochondrial proteins by immunoblot analysis. The photomicrographs demonstrate representative blots of three independent experiments.*

The effect of HO-3538 on the lipid peroxidation, protein oxidation and infarct size in Langendorff-perfused hearts

We assessed protective effect of HO-3538 on ischemia-reperfusion induced damages by determining TBARS formation and carbonyl content of proteins in the perfused heart tissue as a measure of lipid peroxidation and protein oxidation, respectively. Infarct size was estimated after histological staining of thick sections of the perfused hearts. All three parameters were significantly diminished by 5 μM of HO-3538, while amiodarone and SCAV were again somehow less efective (Fig. 23).

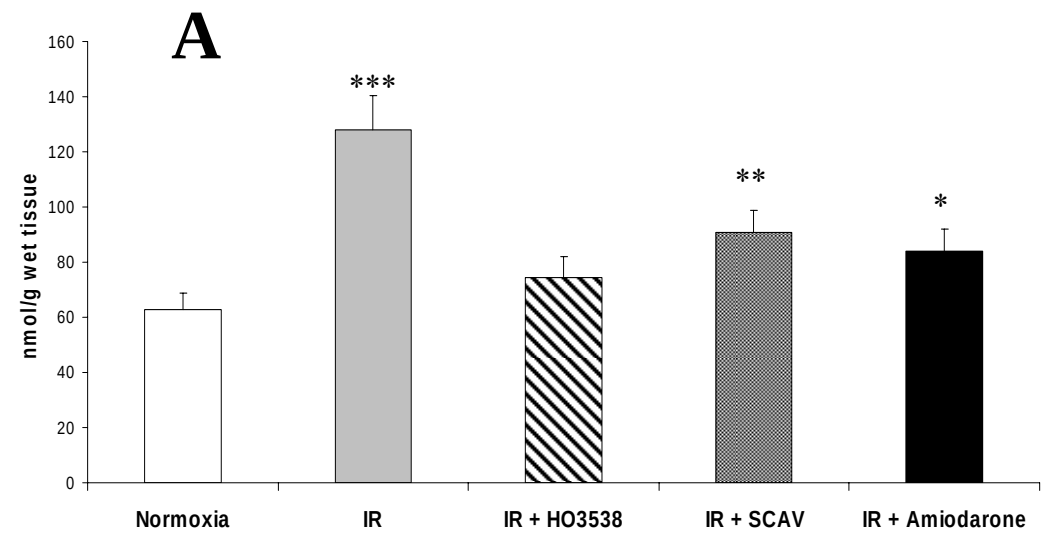
A
nmol/g wet tissue
160
140
120
100
80
60
40
20
0
***
**
*
Normoxia
IR
IR + HO3538
IR + SCAV
IR + Amiodarone

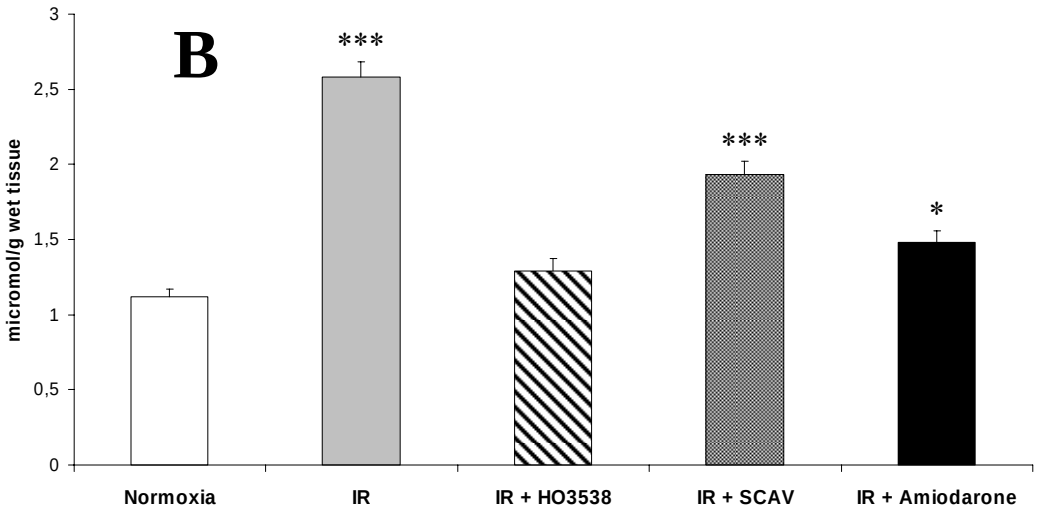
B
micromol/g wet tissue
3
2,5
2
1,5
1
0,5
0
***
***
*
Normoxia
IR
IR + HO3538
IR + SCAV
IR + Amiodarone

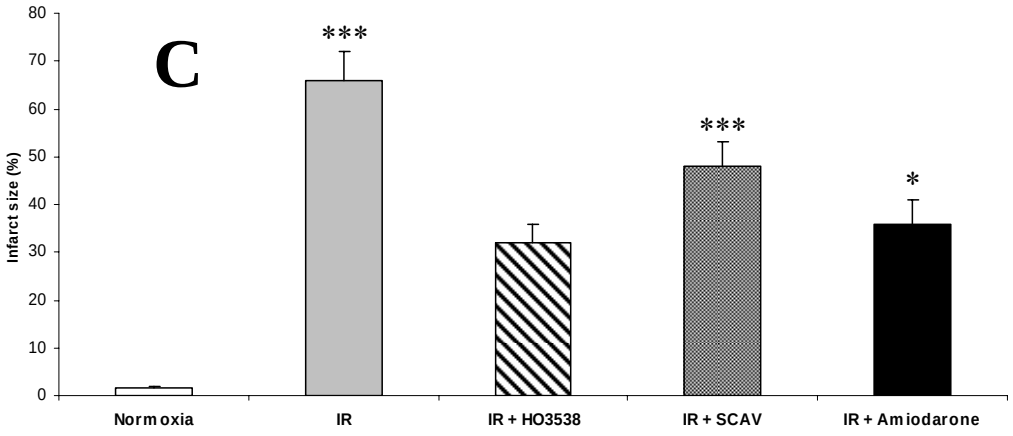
C
Infarct size (%)
80
70
60
50
40
30
20
10
0
***
***
*
Normoxia
IR
IR + HO3538
IR + SCAV
IR + Amiodarone

Fig. 23. The effect of HO-3538 on lipid peroxidation, protein oxidation and infarct size following ischemia reperfusion in Langendorff-perfused hearts. *The hearts were exposed to 30 min of ischemia followed by 15 of reperfusion, then they were subjected to the appropriate measurement.*
(A) Lipid peroxidation was estimated from the formation of thiobarbituric acid reactive substances (TBARS) from homogenates of rat hearts (n = 5 in each group). Using MDA standard, TBARS were calculated as nmol/g of wet tissue.
(B) Protein oxidation was estimated from the protein carbonyl content from homogenates of rat hearts (n = 5 in each group), and expressed as μmol/g wet tissue.
(C) For infarct size measurements, an additional 90-min post-ischaemic reperfusion was employed to rat hearts (n = 5 in each group). The size of the infarcted area was estimated by the TTC staining with volume and weight method as described in the Materials and Methods section.
White column represent normoxic control; grey column represent ischemia-reperfusion, no drug added group; black column represent amiodarone-treated; diagonally striped column represent HO-3538-treated; diagonally chequered column represent SCAV-treated group. Data represent mean ± S.E.M. of five independent experiments.
*Significantly different from HO-3538: *, $p < 0.05$; **, $p < 0.01$); ***, $p < 0.001$.*

Discussion

It is well documented that PARP inhibitors or knockout of the PARP-1 gene protects cells from different types of oxidative stress (37). According to the classical view, this cytoprotection is mainly the result of the prevention of NAD^+ and ATP depletion caused by excessive PARP activation, which is the result of oxidative stress-induced DNA break formation. However, an abundance of recent data indicates that inhibition of poly(ADP-ribosyl)ation is involved in many other processes. For example, PARP may influence the inflammation response via regulation of transcription factors and so by the activation or repression of transcription activity (9). This effect of PARP can be the consequence of direct protein-protein interaction with transcription factors or proteins involved in their regulatory processes; alternatively, it can be the result of the catalytic activity of the PARP enzyme. There are examples for both mechanisms. Transcription factors such as AP-2 (38), B-MYB (39), Oct-1 (40), YY-1 (41), and TEF-1 (42) bind directly to PARP-1, whereas other transcription factors, such as NF-κB (43–46, 30), p53 (47), c-Fos (25, 48), c-Jun (25), and RNA polymerases I (49) and II (50), are regulated by poly(ADP-ribosyl)ation.

We have demonstrated previously that PARP inhibitors induced the phosphorylation and activation of Akt in the liver, lung, and spleen of lipopolysaccharide-treated mice (25, 30), raising the possibility that the biochemical effect of PARP inhibition is mediated, at least partially, through the PI3-kinase/Akt pathway; that is, PARP inhibitors may protect cells by a far more complex mechanism than is expected from NAD^+ and ATP depletion. It is well known that Akt can phosphorylate several regulatory proteins, including GSK3β, caspase-9, BAD, and FKHR (31), by which it can protect cells under stress conditions.

To understand the molecular mechanism of PARP inhibition in oxidative stress, three experimental models were designed; (i) inhibition of PARP by a well characterized PARP inhibitor; (ii) suppression of the PARP-1 protein level by the siRNA technique; and (iii) nonpharmacological inhibition of PARP-1 activity by the transdominant expression of the N-terminal DNA-binding domain of PARP-1 linked to nuclear localization signal and GFP gene sequences. These models could clearly show whether the effect of PARP inhibition was caused by a decreased catalytic activity or the absence of PARP-1 protein. Furthermore, because the design of the siRNA and the PARP-DBD were based on the sequence of nuclear PARP-1, these models could clearly show whether a single-stranded DNA break-induced PARP-1-catalyzed poly(ADP-ribosyl) ation was responsible for the observed effects.

PJ-34 protected the cells in oxidative stress (Fig. 15*A*) and induced Akt phosphorylation and activation as revealed by the phosphorylation of the downstream target, GSK3β (Fig. 17*A*). Although PJ-34 is a well characterized PARP-1 inhibitor, the specificity of a small molecular weight synthetic inhibitor is always questionable because of the presence of several enzymes with mono- and poly(ADP-ribosyl)ating activity in the cells (37). Suppression of the expression of PARP-1 in WRL-68 cells clearly protected the cells from oxidative stress (Fig. 13) and induced Akt phosphorylation and activation indicated by GSK3β phosphorylation (Figs. 15 and 17*B*). Because this method specifically suppressed PARP-1 synthesis, it was clear that PARP-1 was responsible for Akt phosphorylation and activation, although the question remained whether the suppression of PARP-1 catalytic activity or the absence of PARP-1 protein was responsible for the observed phenomenon. The transdominant expression of PARP-DBD inhibited the self-ADP-ribosylation of PARP because binding to single-stranded DNA breaks was essential for the activation of PARP-1, and the PARP-DBD competed with PARP-1 in binding to

single-stranded DNA breaks, only the former did not have catalytic activity. Monitoring intracellular localization of the PARP-DBD construct was enabled because of the presence of GFP in the construct, and the PARP-DBD was found to be present almost exclusively in the nucleus (Fig. 8) so clearly in position to compete with PARP-1. Besides the inhibition of self-ADP-ribosylation of PARP-1, the expression of PARP-DBD significantly protected the cells from H2O2-induced cell death (Fig. 10) and induced Akt phosphorylation and activation (Fig. 11). Taking together all these data, it is unequivocal that Akt activation was the consequence of the inhibition of the single-stranded DNA break-induced PARP-1 activation and not of protein-protein interaction between PARP-1 and other regulatory proteins or of an other mechanism that was regulated by the pharmacological inhibitor.

The significance of the PARP inhibition-induced Akt activation in the survival of cell in oxidative stress can be assessed by the inhibition of PI3-kinase-mediated Akt activation by LY 294002 or by wortmannin. These data show that PI3-kinase inhibitors almost completely blocked the PARP inhibitor-induced cytoprotection and inhibited the PARP inhibitor-induced Akt and GSK phosphorylation; that is, Akt activation played a pivotal role in the cytoprotective effect of PARP inhibitor in oxidative stress under our experimental conditions. Inhibition of Src kinase, which can have a role in Akt activation (51, 52), also decreased Akt phosphorylation and reduced the cytoprotective effect of PARP inhibitor, indicating that Src kinase has been involved in the PARP inhibition-induced Akt activation process. Specificity and possible side effects of a pharmacological agent are always an issue; however, LY 294002 was reported to inhibit all isoforms of PI3-kinase but not to affect other kinases such as protein kinases C and A, mitogen-activated protein kinase, S6 kinase, epidermal growth factor tyrosine kinase, c-Src kinase, PI4-kinase, and diacylglycerol kinase (53). Wortmannin, although affecting myosin light chain kinase, is widely recognized as a selective and specific PI3-kinase inhibitor too with

reportedly no effect on PI4-kinase, protein kinase C, and protein-tyrosine kinases (54). Pp2 was characterized as a selective inhibitor of the Src family of tyrosine kinases (55), so the effect of the above mentioned kinase inhibitors on the PARP inhibition-induced phosphorylation processes and cytoprotection was most likely the result of their main pharmacological effect on their respective kinases rather than a side effect.

Nuclear translocation of mitochondrial apoptosis-inducing factor in response to excess PARP-1 activation triggering chromatin condensation, DNA fragmentation, nuclear shrinkage, and caspase-independent apoptotic cell death was found to represent a major cell death pathway in various neuronal and cardiovascular excitotoxicity and oxidative stress models (35, 56–59). NAD^+ depletion and induction of mitochondrial permeability transition were implicated as intermediate steps linking PARP-1 activation to apoptosis-inducing factor translocation (56). We observed a significant NAD^+ depletion in wild type and pEGFP transfected WRL-68 cells as a consequence of H2O2 treatment which was significantly attenuated by pharmacological or nonpharmacological PARP-1 inhibition (Fig. 14). However, and in contrast to the viability and Akt pathway experiments, the PI3-kinase and Src kinase inhibitors did not counteract, in fact did not affect at all (Fig. 16), the protection of NAD^+ pool by PARP inhibition, which suggests that Src and PI3-kinase activities are not involved in the regulation of the intracellular NAD^+ level and that prevention of NAD^+ depletion and Akt pathway activation are two independent mechanisms of the cytoprotective effect PARP inhibition as is described schematically in Fig. 24. Whether or not nuclear translocation of apoptosis-inducing factor plays a role in our model system is still not clear; however, cell death was predominantly necrotic as revealed by positive propidium iodide and negative fluorescein-labeled annexin V fluorescence (data not shown) and the absence of apoptotic morphology on the fluorescence images (Fig. 18).

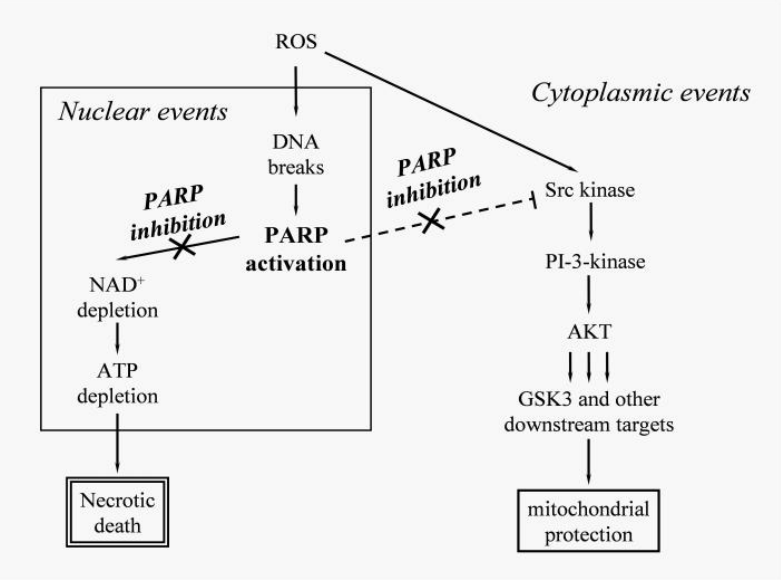

FIGURE 24. Possible molecular mechanism of the cytoprotective effect of PARP inhibition during oxidative stress. *Well documented effects are indicated by solid lines, whereas effects involving yet unidentified mediator(s) or events are represented by a dashed line. Lines with a pointed end denote activation, whereas the one with a flat end indicates inhibition. PARP-1 activation during oxidative stress leads to NAD^+ depletion and via a yet uncharacterized mechanism to inhibition of reactive oxygen species (ROS)-induced PI3-kinase activation, resulting in necrotic cell death. Inhibition of PARP-1 activity suppresses both processes leading to attenuation of NAD^+ depletion, mitochondrial protection, and cell survival.*

Previously, it was reported that PARP inhibitors protect mitochondrial membrane integrity in oxidative stress (32, 33). Because there is evidence for the existence of mitochondrial PARP polymerase (29), when using pharmacological PARP inhibitors, it is hard to determine whether indeed PARP-1 or other PARPs are responsible for the collapse of mitochondrial membrane potential. Using our model system, it was evident that PARP inhibitor PJ-34, suppression of PARP-1 protein expression by siRNA, and the inhibition of single-stranded DNA breakinduced PARP-1 activation by the transdominant expression of PARP-DBD preserved mitochondrial integrity and membrane potential the same way in H2O2-induced oxidative stress (Fig. 18); that is, the enhanced catalytic activity of PARP-1 in oxidative stress is responsible through a mechanism, which is as yet uncharacterized in detail, for the collapse of mitochondrial membrane potential.

It is known that Akt phosphorylates and so inactivates the proapoptotic BAD protein, which process can contribute to the stabilization of the mitochondrial membrane system. Therefore, it was important to determine whether Akt activation was involved in the protection of mitochondrial membrane potential by PARP inhibition. Fig. 18 shows that the PARP inhibition-mediated protection of mitochondrial membrane potential was compromised by PI3-kinase inhibitor LY 294002 (or wortmannin), suggesting that PARP inhibition-induced protection of mitochondrial membrane potential was mediated by the PI3-kinase/ Akt system. A similar effect was observed in the case of Pp2, an Src kinase inhibitor, which was in accord with our previous data showing that Pp2 inhibited the PARP inhibition-induced Akt phosphorylation too. These data show that in oxidative stress, the activation of PARP-1- initiated poly(ADP-ribosyl)ation processes, which somehow negatively influenced Akt activation, were responsible in a significant extent for the collapse of mitochondrial membrane potential. Inhibition of PARP-1 activation by three different methods blocked the excessive poly(ADP-ribosyl)ation, so abolished the suppression of Akt activation, and the activation of Akt participated in the protection of the mitochondrial membrane system (Fig. 24).

Several studies have established the substantial role of opening of the mitochondrial permeability transition pore and free radical production in inducing tissue damage and infarct formation during acute myocardial infarction (15–18). Although ROS may contribute to the opening of the PTP, when natural scavenger molecules (e.g., vitamins C and E) were administered before ischemia in perfused hearts, they failed to present substantial benefit (28). On the other hand, inhibition of the mPT significantly decreased the extent of cell death after ischemia–reperfusion (35). When cyclophilin D knockout mice were subjected to cardiac ischemia–reperfusion, due to the lack of cyclophilin D and thus to the absence of the Ca2+-induced formation of PTP, the infarct size was significantly

lower compared to controls (17). Transient opening of PTP caused by a mild insult induces the release of cytochrome c as well as other proapoptotic proteins, eventually resulting in apoptosis (18,36,37). Reperfusion-induced ROS generation might not be able to induce mPT in the presence of an effective mPT inhibitor; however, it still may cause temporary pore opening and the induction of apoptosis. Therefore, an effective mPT inhibitor that is capable of ROS scavenging in the microenvironment of the PTP may represent an ideal drug candidate for alleviating postinfarct myocardial injuries. HO-3538 indeed inhibited the Ca2+-, tert-butyl hydroperoxide-, and atractyloside-induced mitochondrial swelling in vitro in isolated liver and heart mitochondria (Fig. 2). This effect was inferior to that of cyclosporin A, but was similar to that of amiodarone (4.9 ± 0.5 vs 3.9 ± 0.8 μM), whereas SCAV did not have any effect. More importantly and unlike amiodarone, HO-3538 did not induce swelling on its own up to the concentration of 100 μM. The mPT inhibitory effect of HO-3538 was also demonstrated by detecting the release of proapoptotic proteins from the mitochondria by using immunoblotting and HPLC analysis. By monitoring the mitochondrial membrane potential, we found that at the concentrations at which HO-3538 effectively inhibited mPT it exerted a mild uncoupling effect, too (ED50 = 36.2 ± 3.2 μM). Mild uncoupling could inhibit mPT (38,39) by making the respiratory chain work more efficiently, leading to less leakage of electrons and thus lowering the level of ROS generation (40). All these results show that HO-3538 had beneficial effects on the isolated mitochondria.

It is a widely accepted therapeutic disadvantage of amiodarone that it causes toxic side effects in patients during prolonged treatment (41). Under our experimental conditions, 30 and 100 μM amiodarone significantly reduced viability of H9C2 cardiomyoblasts even after a mere 48-h exposure. However, HO-3538 was not toxic at all under the same conditions as was revealed by using the MTT+ cell-proliferation assay (Fig. 21A). Rather,

it exerted a protective effect that was significantly superior to that of an equimolar concentration of amiodarone against either oxidative stress-induced (Fig. 21B) or etoposide-induced (Fig. 21C) apoptotic cell death in cultured cell lines. Oxidative stress was induced by exposing H9C2 cells to 150 μM H2O2 for 48 h, under which condition the cell death was apoptotic rather than necrotic. H9C2 cells are quite resistant to H2O2, so this H2O2 concentration represented a moderate oxidative stress for them, to which they were exposed for a long time. We compared the cytoprotective effects of HO-3538 with equimolar amounts of various antioxidants, including SCAV, the SOD-mimetic side chain of HO-3538, as well as with amiodarone under these conditions (Fig. 21B). HO-3538 proved to be significantly the most effective among the substances tested, although its antioxidant properties were superior only to that of amiodarone, were about the same as those of vitamin E and N-acetyl cysteine, and were inferior to those of SCAV and vitamin C, as was revealed in a separate experiment (Fig. 21D). In the latter, the cells were exposed to a strong oxidative stress (1 mM H2O2) for 90 min, which induced ROS generation in the cells, but was too short a time to cause considerable cell death. Jurkat cells were used to compare the antiapoptotic properties of amiodarone and HO-3538 assessed by measuring caspase-3 activity. This cell line is a well-established model for detecting the activation of the caspase-dependent apoptotic pathway and, at the concentration of 50 μM, etoposide is not expected to induce considerable ROS formation, providing a suitable setup for the experiment. Both substances decreased the etoposideinduced caspase-3 activity significantly; however, HO-3538 was more effective in this respect than amiodarone (Fig. 21C), even at low concentrations at which amiodarone was not supposed to induce apoptosis [26]. All these results clearly demonstrated the relevance of our working hypothesis because HO-3538 protected the H9C2 cells more effectively than amiodarone (an mPT inhibitor, but poor antioxidant) and vitamin C or SCAV (superior antioxidants to

HO-3538, but no mPT inhibitory properties), and its antiapoptotic effect was superior to that of amiodarone, too. Also, HO-3538 was preferably taken up into the mitochondria, as demonstrated by quantitative mass spectrometry, and localized to a subcellular compartment to exert mitochondrial protection.

Whereas the intrinsic phase of apoptosis is characterized by the release of proapoptotic proteins from the mitochondrial intermembrane space, the permeability transition has important consequences affecting energy production, such as the loss of oxidative phosphorylation capacity due to the failed integrity of the inner membrane, the conversion of complex V (ATP-synthase) from an energy-producing to an energy-consuming complex that consumes glycolytic ATP, and the inhibition of complex I due to the loss of NADH. We evaluated what beneficial consequences could result from the simultaneous inhibition of permeability transition and ROS scavenging on release of.proapoptotic mitochondrial proteins. HO-3538 decresed particulary the release of cyt-c, Endo G, and AIF (Fig. 22) more effectively than amiodarone or SCAV. The latter result suggested that inhibition of mPT is a major factor in the cardioprotective effects of HO-3538. However, the facts that HO-3538 was again more effective than amiodarone and SCAV significantly improved the energy metabolism as well as the cardiac functional parameters emphasize the importance of free radical scavenging in alleviating ischemia–reperfusion-induced damages. ROS produced during the reperfusion period induces lipid peroxidation and DNA damage as well as protein oxidation, which through reactive aldehydes further deteriorate the mitochondria. Under our experimental conditions, HO-3538 significantly improved these parameters as well as decreasing infarct size (Fig. 23). The latter might not represent the ultimate rescue of cardiomyocytes because seemingly smaller infarcts are often merely delayed (42); however, all the other results indicate a clear cytoprotective effect for HO-3538. These results clearly suggest that preservation of the

integrity of the mitochondrial membrane is a significant contributing factor to cytoprotection and cardioprotection, and so it may represent a novel therapeutic target in the management of oxidative stress-related diseases.

Conclusions

1. Several studies demonstrated that the different pharmacological PARP inhibitors have got beficial effects in oxidative stress. We provided evidence that suppression of PARP-1 activation by small molecular weight inhibitor, by siRNA method, or by the transdominant expression of PARP-DBD protected cells from oxidative stress. Since the sequence of the siRNA and the PARP-DBD were based on the sequence of the nuclear PARP-1, the same cytoprotection by the pharmacological and non-pharmacological inhibition has proven that inhibition of the single-stranded DNA break-induced PARP-1 activation was responsible for the protective effect in oxidative stress rather than some side effect of the pharmacological inhibitor.
2. We provided evidence for undermining the classical view that cytoprotection by PARP inhibitors relies exclusively on the preservation of NAD^+ and consequently the ATP stores in oxidative stress. Inhibition of Akt activation by specific inhibitors in a significant extent counteracted the cytoprotective effect of PARP inhibitor, indicating that the PARP inhibition-induced Akt activation was very significantly responsible for the cytoprotective property of PARP inhibitors. We established that the benefit of PARP inhibition is mediated through two different processes in oxidative stress: the preservation of energetics of cells and activation of PI3K/Akt as a well-known survival signaltrasduction pathway.
3. We synthesized numerous paramagnetic and diamagnetic amiodarone derivates and screened their effects on the mitochondrial permeability transition. We found an amiodarone analgue HO-3538 in which an ethyl side chain is substituted with 1-hydroxy-2,2,5,5-tetramethyl-2,5-dihydro-1H-pyrrol-3-

ylmethyl, which has been described to possess SOD-mimetic activity. HO-3538 completely inhibited the Ca2+-induced swelling at low concentration furthermore did not induce mPT at higher concentration.

4. HO-3538, although had a less pronounced free-radical scavenging activity than its SOD-mimetic side chain, and some antioxidants, due to its mPT inhibitory activity combined to its SOD-mimetic activity, was much more effective protective effect in ischemia-reperfusion as well as in oxidative stress than any other compounds tested including amiodarone. This proved that combined mPT inhibitory and free-radical properties whithin the same molecule might represent a useful approach in the therapy of oxidative damage related diseases.

List of Publications

Publications supporting the dissertation:

Antal Tapodi, Balazs Debreceni, Katalin Hanto, Zita Bognar, Istvan Wittmann, Ferenc Gallyas, Jr.,Gabor Varbiro, and Balazs Sumegi: Pivotal role of Akt activation in mitochondrial protection and cell survival by poly(ADP-ribose)polymerase-1 inhibition in oxidative stress***. J Biol Chem.*** 2005 Oct 21;280(42):35767-75. *IF: 5,854*

Zita Bognar , Tamas Kalai , Anita Palfi , Katalin Hanto , Balazs Bognar , Laszlo Mark , Zoltan Szabo , *Antal Tapodi* , Balazs Radnai, Zsolt Sarszegi , Arpad Szanto, Ferenc Gallyas Jr. , Kalman Hideg , Balazs Sumegi, Gabor Varbiro a: A novel SOD-mimetic permeability transition inhibitor agent protects ischemic heart by inhibiting both apoptotic and necrotic cell death. ***Free Radic Biol Med***. 2006 Sep 1;41(5):835-48. *IF: 4,971*

Other publications:

Varbiro G., Toth A., *Tapodi A*., Veres B., Gallyas F., Sumegi B.: The concentration dependent mitochondrial effect of amiodarone. ***Biochem. Pharmacol.*** (2003) 65(7):1115-28. *IF: 2.993*

Gabor Varbiro, Ambrus Toth, *Antal Tapodi*, Zita Bognar, Balazs Veres, Balazs Sumegi, and Ferenc Gallyas, Jr.: Protective effect of amiodarone but not N-desethylamiodarone on postischemic hearts through the inhibition of mitochondrial permeability transition ***J Pharmacol Exp Ther.*** 2003 Nov;307(2):615-25. *IF: 4.337*

Abstracts, posters and presentations supporting the dissertation:

Varbiro, G., Veres, B., Gallyas, F., Tapodi, A., Sumegi, B.: A taxol közvetlen hatása a mitokondriális permeability transitionra és a szabadgyökképződésre. Sümeg, XXXI. Membrán-Transzport Konferencia, 2001. Május 22-25.

Tapodi, A., Veres, B., Varbiro, G., Gallyas, F., Sumegi, B.: Az amiodarone mitokondriális hatásai. Sümeg, XXXI. Membrán-Transzport Konferencia, 2001. Május 22-25.

Jakus P., *Tapodi A*., Varbiro G.: Amiodarone indukálta génexpressziós változások analízise DNS-chip technikával. Pécs, A Pécsi Akadémiai Bizottság Sejtbiológiai Munkabizottságának Doktorandusz Szimpóziuma, 2002. december 11.

Tapodi A., Veres B., *Varbiro G.*, ifj. Gallyas F., Sumegi B.: Az amiodaron bifázisos mitokondriális hatásai. Siófok, X. Sejt- és Fejlődésbiológiai Napok, 2002. Március 27-29.

Gallyas F., Varbiro G., Veres B., *Tapodi A*., Sumegi B.: A Taxol közvetlen módon gyakorol hatást egyes mitokondriális funkciókra. Debrecen, IX. Sejt- és Fejlődésbiológiai Napok, 2001. Január 21-24

Other abstracts, posters and presentations

Varbiro G., *Tapodi A*., Veres B., Gallyas F. Jr., Sumegi B.: The induction of COX-2 expression through an NFkB dependent pathway in liver cells by amiodarone. (Abstract) **Z. Gastroenterologie** 5: (2002)

Varbiro, G., *Tapodi, A*., Veres, B., Gallyas, F., Sumegi, B.: The induction of COX-2 expression through an NFkB dependent pathway in liver cells by amiodarone Balatonaliga, 44rd Annual Meeting of the Hungarian Society of Gastroenterology, 2002. June 4-8.

Veres B., *Tapodi A*., Varbiro G., ifj. Gallyas F., Sumegi B.: PARP-gátlók hatása az LPS indukálta szepszisre. Sümeg, XXXII. Membrán-Transzport Konferencia, 2002. Május 21-24.

Tapodi A., Veres B., Varbiro G., ifj. Gallyas F., Sumegi B.: PARP-gátlók hatása oxidatív stresszben. Sümeg, XXXII. Membrán-Transzport Konferencia, 2002. Május 21-24.

Veres B., Varbiro G., *Tapodi A*., ifj. Gallyas F., Sumegi B.: PARP-gátlók hatása a szeptikus sokkra. Siófok, X. Sejt- és Fejlődésbiológiai Napok, 2002. Március 27-29.

Ifj. Gallyas F., Jun-Ichi Satoh, *Tapodi A*., Varbiro G., Veres B.: Neurotranszmitter szintézis immortalizált sejtvonalakban. Siófok, X. Sejt- és Fejlődésbiológiai Napok, 2002. Március 27-29.

References:

1. Xia, Y., Khatchikian, G., and Zweier, J. L. (1996) *J. Biol. Chem.* 271, 10096–10102

2. Turners, J. F., and Bovanis, A. (1980) *Biochem. J.* 156, 434–444

3. Rowe, G. T., Manson, N. H., Caplan, M., and Hess, M. L. (1983) *Circ. Res.* 53, 584–591

4. Batandier, C., Leverve, X., and Fontaine, E. (2004) *J. Biol. Chem.* 279, 17197–17204

5. Lu, S., Nishimura, K., Hossain, M. A., Jisaka, M., Nagaya, T., and Yokota, K. (2004) *Appl. Biochem. Biotechnol.* 118, 133–153

6. McCord, J. M. (1987) *Fed. Proc.* 46, 2402–2406

7. Werner, E. (2004) *J. Cell Sci.* 117, 143–153

8. Martin, D., Salinas, M., Fujita, N., Tsuruo, T., and Cuadrado, A. (2002) *J. Biol. Chem*. 277, 42943–42952

9. D'Amours, D., Desnoyers, S., D'Silva, I., and Poirier, G. G. (1999) *Biochem. J.* 342, 249–268

10. de Murcia, G., and Menissier de Murcia, J. (1994) *Trends Biochem. Sci.* 19, 172–176

11. Althaus, F. R., Kleczkowska, H. E., Malanga, M., Muntener, C. R., Pleschke, J. M., Ebner, M., and Auer, B. (1999) *Mol. Cell. Biochem.* 193, 5–11

12. Berger, N. A. (1985) *Radiat. Res.* 101, 4–15

13. Jagtap, P., and Szabo, C. (2005) *Nat. Rev. Drug Discov.* 4, 421–440

14. Oleinick, N. L., and Evans, H. H. (1985) *Radiat. Res.* 101, 29–46

15. Ha, H. C., and Snyder, S. H. (1999) *Proc. Natl. Acad. Sci. U. S. A.* 96, 13978–13982

16. Zingarelli, B., Salzman, A. L., and Szabo, C. (1998) *Circ. Res.* 83, 85–94

17. Eliasson, M. J., Sampei, K., Mandir, A. S., Hurn, P. D., Traystman, R. J., Bao, J., Pieper,
A., Wang, Z. Q., Dawson, T. M., Snyder, S. H., and Dawson, V. L. (1997) *Nat. Med.* 3, 1089–1095

18. Endres, M., Wang, Z. Q., Namura, S., Waeber, C., and Moskowitz, M. A. (1997) *J. Cereb. Blood Flow Metab.* 17, 1143–1151

19. Liaudet, L., Pacher, P., Mabley, J. G., Virag, L., Soriano, F. G., Hasko, G., and Szabo, C.
(2002) *Am. J. Respir. Crit. Care Med.* 165, 372–377

20. Soriano, F. G., Liaudet, L., Szabo, E., Virag, L., Mabley, J. G., Pacher, P., and Szabo, C.
(2002) *Shock* 17, 286–292

21. Szabo, C., Lim, L. H., Cuzzocrea, S., Getting, S. J., Zingarelli, B., Flower, R. J., Salzman,
A. L., and Perretti, M. (1997) *J. Exp. Med.* 186, 1041–1049
22. Pieper, A. A., Brat, D. J., Krug, D. K., Watkins, C. C., Gupta, A., Blackshaw, S., Verma,
A., Wang, Z. Q., and Snyder, S. H. (1999) *Proc. Natl. Acad. Sci. U. S. A.* 96, 3059–3064
23. Masutani, M., Suzuki, H., Kamada, N., Watanabe, M., Ueda, O., Nozaki, T., Jishage, K.-i., Watanabe, T., Sugimoto, T., Nakagama, H., Ochiya, T., and Sugimura, T. (1999) *Proc. Natl. Acad. Sci. U. S. A.* 96, 2301–2304
24. Burkart, V., Wang, Z. Q., Radons, J., Heller, B., Herceg, Z., Stingl, L., Wagner, E. F., and
Kolb, H. (1999) *Nat. Med.* 5, 314–319
25. Veres, B., Radnai, B., Gallyas, F., Jr., Varbiro, G., Berente, Z., Osz, E., and Sumegi, B. (2004) *J. Pharmacol. Exp. Ther.* 310, 247–255
26. Palfi, A., Toth, A., Kulcsar, G., Hanto, K., Deres, P., Bartha, E., Halmosi, R., Szabados, E., Czopf, L., Kalai, T., Hideg, K., Sumegi, B., and Toth, K (June, 2005) *J. Pharmacol. Exp. Ther.* 10.1124/jpet.105.088336
27. Murriel, C. L., Churchill, E., Inagaki, K., Szweda, L. I., and Mochly-Rosen, D. (2004) *J. Biol. Chem.* 279, 47985–47991
28. Halmosi, R., Berente, Z., Osz, E., Toth, K., Literati-Nagy, P., and Sumegi, B. (2001) *Mol. Pharmacol.* 59, 1497–1505
29. Du, L., Zhang, X., Han, Y. Y., Burke, N. A., Kochanek, P. M., Watkins, S. C., Graham, S. H., Carcillo, J. A., Szabo, C., and Clark, R. S. (2003) *J. Biol. Chem.* 278, 18426–18433
30. Veres, B., Gallyas, F., Jr., Varbiro, G., Berente, Z., Osz, E., Szekeres, G., Szabo, C., and
Sumegi, B. (2003) *Biochem. Pharmacol.* 65, 1373–1382
31. Scheid, M. P., and Woodgett, J. R. (2001) *Nat. Rev Mol. Cell Biol.* 2, 760–768
32. Virag, L., Salzman, A. L., and Szabo, C. (1998) *J. Immunol.* 161, 3753–3759
33. Hong, S. J., Dawson, T. M., and Dawson, V. L. (2004) *Trends Pharmacol. Sci.* 25, 259–264
34. Kim, J. W., Won, J., Sohn, S., and Joe, C. O. (2000) *J. Cell Sci.* 113, 955–961
35. Xiao, C. Y., Chen, M., Zsengeller, Z., Li, H., Kiss, L., Kollai, M., and Szabo, C. (2005) *J. Pharmacol. Exp. Ther.* 312, 891–898

36. Shah, G. M., Poirier, D., Duchaine, C., Brochu, G., Desnoyers, S., Lagueux, J., Verreault,
A., Hoflack, J.-C., Kirkland, J. B., and Poirier, G. G. (1995) *Anal. Biochem*. 227, 1–13
37. Virag, L., and Szabo, C. (2002) *Pharmacol. Rev.* 54, 375–429
38. Kannan, P., Yu, Y., Wankhade, S., and Tainsky, M. A. (1999) *Nucleic Acids Res.* 27, 866–874
39. Cervellera, M. N., and Sala, A. (2000) *J. Biol. Chem.* 275, 10692–10696
40. Nie, J., Sakamoto, S., Song, D., Qu, Z., Ota, K., and Taniguchi, T. (1998) *FEBS Lett.* 424, 27–32
41. Oei, S. L., Griesenbeck, J., Schweiger, M., Babich, V., Kropotov, A., and Tomilin, N. (1997) *Biochem. Biophys. Res. Commun.* 240, 108–111
42. Butler, A. J., and Ordahl, C. P. (1999) *Mol. Cell. Biol.* 19, 296–306
43. Hassa, P. O., Covic, M., Hasan, S., Imhof, R., and Hottiger, M. O. (2001) *J. Biol. Chem.*
276, 45588–45597
44. Ullrich, O., Distel, A., Eyupoglu, I. Y., and Nitsch, R. (2001) *Nat. Cell Biol.* 3, 1035–1042
45. Kameoka, M., Ota, K., Tetsuka, T., Tanaka, Y., Itaya, A., Okamoto, T., and Yoshihara, K. (2000) *Biochem. J.* 346, 641–649
46. Chang, W. J., and Alvarez-Gonzalez, R. (2001) *J. Biol. Chem*. 276, 47664–47670
47. Wesierska-Gadek, J., and Schmid, G. (2001) *Cell. Mol. Biol. Lett.* 6, 117–140
48. Amstad, P. A., Krupitza, G., and Cerutti, P. A. (1992) *Cancer Res.* 52, 3952–3960
49. Muller, W. E., and Zahn, R. K. (1976) *Mol. Cell. Biochem.* 12, 147–159
50. Taniguchi, T., Suzuki, S., and Shizuta, Y. (1985) *Biochem. Biophys. Res. Commun.* 127,
526–532
51. Esposito, G., Ligresti, A., Izzo, A. A., Bisogno, T., Ruvo, M., Di Rosa, M., Di Marzo, V.,
and Iuvone, T. (2002) *J. Biol. Chem.* 277, 50348–50354
52. Cui, Q. L., Zheng, W. H., Quirion, R., and Almazan, G. (2005) *J. Biol. Chem.* 280, 8918–8928
53. Vlahos, C. J., Matter, W. F., Hui, K. Y., and Brown, R. F. (1994) *J. Biol. Chem.* 269, 5241–5248

54. Powis, G., Bonjouklian, R., Berggren, M. M., Gallegos, A., Abraham, R., Ashendel, C., Zalkow, L., Matter, W. F., Dodge, J., and Grindey, G. (1994) *Cancer Res.* 54, 2419–2423

55. Hanke, J. H., Gardner, J. P., Dow, R. L., Changelian, P. S., Brissette, W. H., Weringer, E. J., Pollok, B. A., and Connelly, P. A. (1996) *J. Biol. Chem.* 271, 695–701

56. Alano, C. C., Ying, W., and Swanson, R. A. (2004) *J. Biol. Chem.* 279, 18895–18902

57. Yu, S. W., Wang, H., Poitras, M. F., Coombs, C., Bowers, W. J., Federoff, H. J., Poirier,
G. G., Dawson, T. M., and Dawson, V. L. (2002) *Science* 297, 259–263

58. Komjati, K., Mabley, J. G., Virag, L., Southan, G. J., Salzman, A. L., and Szabo, C. (2004)
Int. J. Mol. Med. 13, 373–382

59. Chen, M., Zsengeller, Z., Xiao, C. Y., and Szabo, C. (2004) *Cardiovasc. Res.* 63, 682–688

Acknowledgement

I would like to thank prof. Dr. Balazs Sümegi the support, and guidance I received.

I would like to thank dr. Ferenc Gallyas Jr., associate professor the cooperation, assistance and advices.

I would like to thank dr. Gabor Varbiro, dr. Zita Bognar and dr. Katalin Hanto, colleagues and friends cooperation and completeing my work.

I would also like thank the technical help I recieved fom Isvanné Pásztor, Helena Halász, László Girán and Bertalan Horváth.

And last but not least I would like to thank my family the support and encouragment for completing my work.